View metadata, citation and similar papers at core.ac.uk

brought to you by CORE

provided by T-Stór

Title: MicroRNA regulation of bovine monocyte inflammatory and metabolic networks in an *in vivo* infection model.

Authors:

Nathan Lawless[*§]

Timothy A. Reinhardt [†]

Kenneth Bryan [*]

Mike Baker [‡]

Bruce Pesch [†]

Duane Zimmerman [†]

Kurt Zuelke [**]

Tad Sonstegard [§§]

Cliona O'Farrelly [§]

John D. Lippolis [†]

David J. Lynn [*]

Affiliations:

[*]Animal & Bioscience Research Department, Animal & Grassland Research and Innovation Centre, Teagasc, Grange, Dunsany, Co. Meath, Ireland.

[§]School of Biochemistry & Immunology, Trinity College, Dublin 2, Ireland.

[†] USDA-ARS, National Animal Disease Center, Ames, IA, 50010 USA.

© The Author(s) 2013. Published by the Genetics Society of America.

[‡] Iowa State University, DNA Facility, Molecular Biology Building, Ames, IA, 50010 USA.

[**] Australian Animal Health Laboratory, CSIRO, East Geelong VIC 3219, Australia

[§§] USDA-ARS, Beltsville, MD, 20705-1350, USA.

NCBI GEO database and assigned the identifier (GSE51858).

Short title: mRNA & miRNA expression in bovine monocytes.

Corresponding Authors: David Lynn, Animal & Bioscience Research Department, Animal & Grassland Research and Innovation Centre, Teagasc, Grange, Dunsany, Co. Meath, Ireland. +353(0)469026729, david.lynn@teagasc.ie. John Lippolis, USDA-ARS, National Animal Disease Center, Ames, IA, 50010 USA, +5153377446, john.lippolis@ars.usda.gov.

Infection/Innate immunity/RNAseq/microRNA/Transcriptional networks

ABSTRACT

Bovine mastitis is an inflammation-driven disease of the bovine mammary gland that costs the global dairy industry several billion dollars per annum. Because disease susceptibility is a multi-factorial complex phenotype, an integrative biology approach is required to dissect the molecular networks involved. Here, we report such an approach, using next generation sequencing combined with advanced network and pathway biology methods to simultaneously profile mRNA and miRNA expression at multiple time-points (0, 12, 24, 36 and 48h) in both milk and blood FACS-isolated CD14+ monocytes from animals infected *in vivo* with *Streptococcus uberis*. More than 3,700 differentially expressed (DE) genes were identified in milk-isolated monocytes (MIMs), a key immune cell recruited to the site of infection during mastitis. Up-regulated genes were significantly enriched for inflammatory pathways, while down-regulated genes were enriched for non-glycolytic metabolic pathways. Monocyte transcriptional changes in the blood, however, were more subtle but highlighted the impact of this infection systemically. Genes up-regulated in blood-isolated-monocytes (BIMs) showed a significant association with interferon and chemokine signalling. Furthermore, twenty-six miRNAs were differentially expressed in MIMs and three in BIMs. Pathway analysis revealed that predicted targets of down-regulated miRNAs were highly enriched for roles in innate immunity (FDR < 3.4E-8) in particular TLR signalling, while up-regulated miRNAs preferentially targeted genes involved in metabolism. We conclude that during *S. uberis* infection miRNAs are key amplifiers of monocyte inflammatory response networks and repressors of several metabolic pathways.

INTRODUCTION

Bovine mastitis is an inflammation-driven disease of the bovine mammary gland that is associated with very significant costs to the global dairy industry. In Europe this cost is estimated to be approximately €2 billion/annum (Wells *et al.*, 1998), with similar figures available for the USA (Jones, 2009). Causative agents of mastitis infection include, but are not limited to coliforms (*E. coli),* Streptococci (*S. uberis*) and Staphylococci *(S. aureus*). *Streptococcus uberis* is now ranked amongst the most prevalent mastitis causing pathogens throughout the EU and in North America (Reinoso *et al.*, 2011; Ward *et al.*, 2009).

Mastitis develops as bacteria entering the udder via the teat canal stimulate a pathological form of inflammation. Bacteria encounter epithelial cells lining the mammary gland stimulating a local inflammatory response which facilitates their transport across the epithelial barrier where they are detected by resident immune cells, such as monocytes. Both cell types constitutively express surface pathogen recognition molecules such as Toll-like Receptors (TLRs) enabling them to function in a sentinel capacity. Invasive *S. uberis* triggers TLR2 and 4 mobilising local and systemic inflammatory mediators (Bannerman *et al.*, 2004; Moyes *et al.*, 2009). Typically, chemokines, interleukins (ILs) and tumour necrosis factor α (TNF) initiate local physiological changes in vascular permeability, cell differentiation, and apoptosis. Concurrently, systemic innate immune changes provoke acute phase protein (APP) production which is distributed systemically to suppress the spread of bacteria locally (Mitterhuemer *et al.*, 2010). During this phase, immune cells are recruited to the point of infection (Rinaldi *et al.*, 2010). Monocytes are released from the bone marrow into the circulatory system and eventually reach the mammary gland

via chemokine ligand-mediated cell migration. There they differentiate into macrophage and dendritic cell populations (Dong *et al.*, 2013; Shi & Pamer, 2011). Neutrophils make up the majority of immune cells in an infected gland during an infection. Neutrophils are tasked with directly clearing invasive bacteria via phagocytosis or neutrophil extracellular traps (NETS) and subsequently aid in resolution of inflammation (Lippolis *et al.*, 2006; Reinhardt *et al.*, 2013). Once recruited to the site of infection, monocytes and neutrophils orchestrate antimicrobial activity to control bacterial spread and resolve the infection (Dong *et al.*, 2013; Serbina *et al.*, 2008). Immune cells and other somatic cells can be detected in the milk of infected animals and the counts of the number of such somatic cells per ml, called the somatic cell count, is an indicator of mastitis (Jones, 2009).

The local immune response in mammary tissues has been examined by several approaches both *in vivo* & *in vitro*. Candidate gene based approaches and microarray technology have determined that over 2,000 genes spanning immunity, metabolism, & tissue remodelling are active during mastitis (Mitterhuemer *et al.*, 2010; Moyes *et al.*, 2009; Swanson *et al.*, 2009). Modest data is, however, available examining transcriptional activity in either milk or blood monocytes from infected animals (Prgomet *et al.*, 2005) and little is known regarding the role microRNAs play in regulating these responses.

MicroRNAs (miRNAs) are small, non-coding RNAs, which play a key role in the regulation of innate and adaptive immunity as post-transcriptional regulators of gene expression (O'Connell *et al.*, 2010). They have been shown to regulate immune function in several cell types. Neutrophil senescence, for example, is regulated by a discrete miRNA repertoire (Ward *et al.*, 2011). Naïve mouse B cells are indirectly regulated by miR-155 via histone deacetylase 4 repression, while naive CD4+ T cell

differentiation and function is regulated by global changes in miRNAs (Bronevetsky *et al.*, 2013; Sandhu *et al.*, 2012). In a recent study, we concluded that miRNAs likely play a key role in regulating the innate immune response in mammary epithelial cells to a bovine mastitis pathogen *in vitro* (Lawless *et al.*, 2013).

Although miRNA expression is abundant in numerous bovine tissues, genome-wide studies elucidating the regulatory roles of miRNAs in bovine immunity are limited (Coutinho *et al.*, 2007; Jin *et al.*, 2009; Xu *et al.*, 2009). Furthermore, no bovine studies to date have applied next generation sequencing (NGS) to examine global miRNA expression in immunity and infection *in vivo*. In this study, we report a NGS approach to profile the expression of bovine miRNAs & mRNAs at multiple time-points in milk and blood isolated CD14+ monocyte cells isolated from Holstein Friesians infected *in vivo* with *Streptococcus uberis* a causative agent of bovine mastitis.

MATERIALS AND METHODS

Animals

10 female Holstein Friesians in the middle of their first lactation period, aged between 26-30 months, and 3-5 months post-partum, were selected for this study. The trial was conducted at the USDA National Animal Disease Centre (NADC) Ames, Iowa. All animals had a medical history that was free from mastitis. The National Animal Disease Centre's Animal Care and Use Committee approved all procedures used in this study.

Infection Protocol

Five animals were infected via the teat canal of the right front quarter with approximately 500 colony forming units (CFU) of a mastitis-causing pathogen, *Streptococcus uberis* 0140, in 10 ml of saline. Five control animals were inoculated with saline only. Milk and blood samples were obtained from each animal at 0, 12, 24, 36 and 48 hrs post-infection (or mock infection) as described below. At each time point rectal temperature, total volume of milk, somatic cell count, bacterial counts, ambient temperature, humidity, and additional observations were recorded for each animal. Bacterial counts were determined from 5 ml milk samples collected aseptically from the infected quarter. Milk was serially diluted in sterile phosphate-buffered saline and spread on blood agar plates, then incubated for 24 h at 37 °C. Following incubation, plates were examined for bacterial growth and colony forming units (CFU) per ml were determined.

Cell Extraction from Milk

Milk was collected using a sterilised quarter milker from infected and control animals at each time-point. The total volume of milk was noted. 5ml of milk was isolated for milk bacteriology. The remaining milk was then diluted into Hanks balanced salt solution w/o Ca, Mg, Phenol red (HBSS) + 10 mM EDTA. The mixture was inverted several times, and transferred to a 1l centrifuge bottle and centrifuged in a fixed angle rotor at 10,000 x g for 30 mins. After centrifugation the supernatant was poured off and the pellets were resuspended in 150 ml of HBSS + 5 mM EDTA. The resuspended pellets were then transferred to fresh centrifuge tubes and spun at 2500 x g for 30 mins. After the second spin, the supernatant was poured off and the pellet from each sample was resuspended in 20ml of RPMI 1640 + 1 mM Sodium Pyruvate + 2 mM l Glutamine + 50 ug/ml Gentamycin + 10% FBS (cRPMI) (Sigma-Aldrich, Steinheim, Germany). The 20 ml of cell suspension was divided into 2 x 10 ml aliquots in 15ml conical centrifuge tubes. The cells were pelleted by centrifuge @ 650 x g. After this spin the pellets were pooled into 4ml of cRPMI and were labelled for cell sorting. The cells were counted by trypsin blue exclusion (Careforde, IL, USA) to determine the cell count.

Cell Extraction from Blood

At each time-point, animals were lead into a crush, and 2x60cc syringes of blood were extracted by venipuncture and immediately placed on ice. The total volume of blood and total number of cells in blood were determined using a haemocytometer. Blood was spun for 20 mins at 1200 x g. The buffy coat was observed between serum and

red blood cell phase, and removed. Contaminating red blood cells were lysed by adding 1 volume lysis solution (10.6mM Na2HPO4; 2.7mM NaH2PO4) and inverting the tubes several times immediately followed by adding ½ volume restore solution (10.6mM Na2HPO4; 2.7mM NaH2PO4; 460mM NaCl) and inverting the tubes. The buffy coat was then spun for 10 mins at 650 x g, and the red supernatant was poured off. Cells were re-suspended in red blood cell lysis solution and then restore solution again as above. Cell were spun for a further 5 mins at 650 x g, and re-suspended in 5-10 ml of media.

Isolation of CD14+ Monocytes by Flow Cytometry

Milk and blood derived CD14+ monocytes were isolated by Fluorescence-activated cell sorting (FACS). Briefly, cells were labelled with monoclonal anti-bovine CD14 (Clone CAM36A, VMRD, Pullman, WA, USA) and a PE-conjugated anti-mouse IgG1 antibody (Southern Biotechnology, Birmingham, AL, USA). Labelled cells were separated based on fluorescence intensity using the BD FACS Aria Cell Sorting System (BD Biosciences, CA, USA). Cells with greater than 95% purity were isolated from the milk and peripheral blood of each animal.

mRNA Extraction

The mirVana^{TM} RNA Isolation Kit (Ambion, TX, USA.) was used to extract total RNA from FACS-isolated cell populations. Procedures were performed according to the manufacturer's protocol (File S1). RNA was quantified, and integrity confirmed

using an Agilent RNA Kit on a 2100 Bioanalyzer platform (Agilent Technologies, CO, USA) (File S1).

miRNA Extraction

MicroRNA was extracted using mirPremier^{TM} microRNA Isolation Kits (Sigma-Aldrich, Steinheim, Germany). Procedures were performed according to the manufacturer's protocol (File S1). Small RNA was quantified using an Agilent small RNA Kit on a 2100 Bioanalyzer platform (File S1).

mRNA Library Generation

One hundred indexed mRNA libraries (50 blood monocyte and 50 milk monocyte libraries) were prepared for cluster generation using TruSeq v2 RNA sample preparation kits (Illumina, CA, USA). Procedures were performed according to the manufacturer's protocol (File S1). The finished libraries were validated on an Agilent Bioanalyzer 2100 using an Agilent DNA-1000 chip (Agilent, CO, USA), at which point they were loaded for cluster generation. The samples were sequenced on an Illumina HiSeq 2000 at the Iowa State Sequencing Centre (50bp single-end). Infected and control samples (n =100) were randomised across four flow cells (i.e. 3 or 4 samples multiplexed per lane) to avoid confounding flow cell/lane effects (Auer & Doerge, 2010). The barcode compatibility chart provided with the TruSeq RNA sample preparation kit was adhered to when pooling libraries. Fastq files were produced using the CASAVA 1.8 pipeline.

mRNAseq Analysis

100 fastq files were generated containing the sequencing data for each of the 100 mRNAseq libraries. The quality and number of the reads for each sample were then assessed using FASTQC v0.10.0 (http://www.bioinformatics.bbsrc.ac.uk/projects/fastqc/). Each sample was then put through a number of quality control filters. Firstly, reads were filtered using the fastq Illumina filter v0.1 (http://cancan.cshl.edu/labmembers/gordon/fastq_illumina_filter/), which removes reads from the fastq files which were flagged as not passing the Illumina CASAVA pipeline filters. Cutadapt v1.2 (http://code.google.com/p/cutadapt/) was used to trim the adaptors from reads where necessary. The remaining reads were then further filtered using the fastq quality filter package (http://hannonlab.cshl.edu/fastx_toolkit/) v0.0.13.2. Reads where at least 70% of the bases had a Phred score < 20 were removed. Reads passing all the above filters were also trimmed at their ends to remove low quality bases (Phred score < 20). Reads which were < 20 nt after trimming were discarded. Reads which passed all quality control steps were then aligned to the bovine genome (UMD3.1 assembly (Zimin *et al.*, 2009)) using TopHat v 2.0.8 (Trapnell *et al.*, 2009) allowing 1 mismatch. Reads that did not uniquely align to the genome were discarded. HTSeq-count version 0.5.3p3 (http://wwwhuber.embl.de/users/anders/HTSeq/doc/overview.html) using the union model was used to assign uniquely aligned reads to Ensembl (v69) annotated bovine genes.

Differential Gene Expression Analysis

Data was normalised across libraries using the trimmed mean of M-values (TMM) normalisation method (Bullard *et al.*, 2010). The R (version 2.15.2) Bioconductor package EdgeR (v2.4.6) (Robinson *et al.*, 2010), which uses a negative binomial distribution model to account for both biological and technical variability was applied to identify statistically significant differentially expressed genes. Any samples that had < 5 million uniquely aligning reads were removed from further analysis. Only genes that had at least 1 count per million in at least 3 samples were analysed for evidence of differential gene expression. The analysis was undertaken using moderated tagwise dispersions. Differentially expressed genes were defined as having a fold change in gene expression > 1.5 and a Benjamini and Hochberg corrected FDR of < 0.05 (Benjamini & Hochberg, 1995).

Hierarchical Clustering

Hierarchical clustering of milk and blood mRNA normalised read counts were carried out in the R (version 2.15.2) *hclust* package. Heatmaps were generated using the R *heatmap* package.

Gene Ontology and Pathway Analysis

The R (version 2.15.2) Bioconductor package GOseq (version 1.10.0) which corrects for gene length bias (Young *et al.*, 2010) was used to identify over-represented pathways using pathway annotation imported from the Kyoto Encyclopedia of Genes

and Genomes (KEGG) (Kanehisa *et al.*, 2007) database. KEGG disease pathways were excluded to focus the analysis on primary signalling pathways. Pathways were considered significantly over-represented with an FDR < 0.05. Pathway analysis was undertaken using Ensembl predicted human 1:1 orthologs of the bovine differentially expressed genes.

Additionally, we manually generated two pathway annotations that were of interest but not annotated in detail in KEGG; the "inflammasome" and "interferon" pathways. Gene IDs for these pathways were sourced from SA biosciences (Qiagen) RT² Profiler™ PCR Array Human Interferon and Receptors (PAHS-064A), and RT² Profiler™ PCR Array Human Inflammasome (PAHS-097A) annotations. The interferon pathway consisted of 84 genes (Table S1) whose expression is controlled by or involved in cell signalling mediated by interferon ligands and receptors, while the inflammasome pathway consisted of 95 key genes (Table S1) involved in the function of inflammasomes, protein complex's involved in innate immunity, as well as general NOD-like receptor (NLR) signalling.

Network Analysis Methods

To generate molecular interaction networks, the human 1:1 orthologs of bovine genes that were differentially expressed, at least one of the four time-points, in milk isolated monocytes (MIMs) from *S. uberis* infected animals, were uploaded to InnateDB (www.innatedb.com) (Lynn *et al.*, 2008). InnateDB is one of the most comprehensive databases of all human and mouse experimentally-supported molecular interactions (>300,000 interactions in July 2013) but also specifically includes annotation on more than 19,000 manually curated human and mouse innate

immunity relevant interactions, many of which are not present in any other database (Lynn *et al.,* 2010). Networks were visualized using Cytoscape 2.8.2 (Shannon *et al.*, 2003).

The network was analysed using the cytoHubba plugin (Lin *et al.*, 2008) for Cytoscape 2.8.2 (Shannon *et al.*, 2003) to identify network hubs and bottlenecks using default parameters. The jActiveModules plugin (Ideker *et al.*, 2002) in Cytoscape 2.8.2 (Shannon *et al.*, 2003) was also used to identify high-scoring differentially expressed sub-networks (Overlap Threshold = 0.3; Search depth = 3; Number of modules = 5; "Regional Scoring" and "Adjust score for size" both enabled). The InnateDB pathway analysis tool was used to identify over-represented pathways among module genes.

miRNA Library Generation

One hundred indexed miRNA libraries (50 blood and 50 milk monocyte libraries) were also prepared for cluster generation and sequencing using the TruSeq Small RNA sample preparation kit. These miRNA libraries were prepared from the same samples that the mRNAseq libraries were prepared. Procedures were performed according to the manufacturer's protocol (File S1). The finished libraries were validated on an Agilent Bioanalyzer 2100 using an Agilent DNA high sensitivity chip (Agilent, CO, USA), at which point they were loaded for cluster generation. The samples were sequenced on an Illumina HiSeq 2000 (50bp single-end). Infected and control samples (n =100) were randomised across three flow cells (i.e. 7 or 8 samples multiplexed per lane), to avoid confounding flow cell/lane effects (Auer & Doerge, 2010). Fastq files were produced using the CASAVA 1.8 pipeline. In a few cases, the

sequenced miRNA libraries were found to be adaptor contaminated. These libraries were re-purified and re-sequenced. The list of re-sequenced samples can be found in the supplementary data section (Table S2).

miRNAseq Analysis

Preliminary quality control analysis of the 100 miRNAseq fastq files was again carried out with FASTQC software v0.10.0 (http://www.bioinformatics.babraham.ac.uk/projects/fastqc/). Cutadapt v1.2 (code.google.com/p/cutadapt/) was then used to trim 3' adaptor sequences. Reads which were shorter than 18 nucleotides after trimming were discarded. Trimmed reads were then further filtered using the fastq quality filter (http://hannonlab.cshl.edu/fastx_toolkit/) v0.0.13.2. Reads where at least 70% of the bases had a Phred score < 20 were removed (Cock *et al.*, 2010). Finally, reads passing all the above filters were also trimmed at their ends to remove low quality bases (Phred score < 20). Reads which successfully passed filtering were aligned to the bovine genome (UMD3.1) using novoalign v2.08.03 in miRNA mode (http://www.novocraft.com) allowing 1 mismatch. Non-uniquely aligning reads were discarded. HTSeq version 0.5.3p3 (http://www-huber.embl.de/users/anders/HTSeq/doc/overview.html) using the union model was used to assign uniquely aligned reads to miRBase v 19 miRNA annotation (Kozomara & Griffiths-Jones, 2011). The sequencing data from this publication have been submitted to the NCBI GEO database and assigned the identifier (GSE51858).

Differential miRNA Expression Analysis

Prior to assessing differential expression, miRNAseq count data were first normalised across libraries using either the trimmed mean of M-values (TMM) normalisation method (Robinson *et al.*, 2010) or upper-quantile normalisation (Bullard *et al.*, 2010). Differential expression analysis of miRNAseq data has been shown to be sensitive to the normalisation approach implemented (Garmire & Subramaniam, 2012). To address this issue, we identified differentially expressed miRNAs in two alternatively normalised datasets; TMM-normalised (Robinson *et al.*, 2010), upper-quantile normalised and with no normalisation. Only miRNAs which were identified as differentially expressed across all three datasets were considered further i.e. the differential expression of these miRNAs was robust to the normalisation procedure (Lawless *et al.*, 2013). Any samples that had < 2 million uniquely aligning reads were removed from further analysis. The R (version 2.15.2) Bioconductor package EdgeR (v2.4.6) (Robinson *et al.*, 2010) was applied to identify statistically significant differentially expressed miRNAs. The analysis was undertaken using moderated tagwise dispersions. Differentially expressed miRNAs were defined as having a Benjamini and Hochberg corrected P value of < 0.05 (Benjamini & Hochberg, 1995).

Co-expression and Target Analysis of miRNA and mRNA Data

To identify mRNAs that were potentially regulated by differentially expressed (DE) miRNAs in MIMs, we first sought to calculate Pearson correlations, using the Apache commons Java statistics library, between all DE miRNA expression in reads per million (rpm) and all mRNA expression (TMM normalised read counts) over the

time-course. A correlation matrix was constructed consisting of 26 (DE miRNAs) x 24,616 (All mRNAs) correlation coefficients. The resulting correlation matrix was then filtered to remove both non-significant correlations (critical value for Pearson's correlation for this matrix is r = -0.3116) and those inverse correlations that were not supported by miRanda predicted miRNA-target pairs (miRanda v3.3a). The mRNAs predicted to be targeted (i.e. had a significant anti-correlation relationship in the expression of the mRNA and the miRNA, plus a predicted seed target) by either up- or down-regulated miRNAs were then selected for pathway analysis. Two-dimensional cluster analysis and visualization, using R version 2.15.3 *hclust* and *heatmap.plus* packages, was then applied to the filtered correlation matrix.

Pathway Analysis of Predicted miRNA Target Genes

Target genes of differentially expressed miRNAs were submitted to InnateDB (Lynn *et al.*, 2008) for pathway analysis. Genes were submitted in two groups; those that were targets of up-regulated miRNAs, and those that were targets of down-regulated miRNAs. Significant pathways were calculated based on hypergeometric analysis, pathways of interest were defined as having a Benjamini and Hochberg corrected P value of < 0.05 (Benjamini & Hochberg, 1995).

Novel miRNA Discovery

Using the software package miRDeep2 v0.0.5 (Mackowiak, 2011) we examined whether milk/blood monocytes encoded for miRNAs not yet annotated in the bovine genome. We further parsed this data using a number of different parameters to

identify those novel miRNAs that have the highest likelihood of being true positives as described previously (Lawless *et al.*, 2013). Specifically, we identified those predictions where both the mature and star stands were expressed with a minimum of 5 reads each; where miRDeep2 predicted that the miRNA had > 90% probability of being a true positive; where the hairpin structure had a significant Randfold p-value and where the novel miRNA was independently predicted in two or more different miRNAseq samples.

RESULTS

The Kinetics of S. uberis Infection in vivo

To investigate the host monocyte transcriptional and post-transcriptional response to a mastitis-causing pathogen *in vivo*, five Holstein Friesian animals were infected via the teat canal with approximately 500 CFU of *Streptococcus uberis* 0140, in 10 ml of saline. Five control animals were inoculated with saline only. Blood and milk samples were taken at 0, 12, 24, 36 and 48 hours post infection (hpi) and CD14+ monocytes were isolated by FACS (Figure 1). The infection was monitored using recorded milk bacterial counts (CFU/ml) and somatic cell counts (per ml) at each of the five time points for each animal (control & infected). On average, bacterial counts peaked in the infected animals at 24hpi, whereas no change was observed in the uninfected controls. There was, however, significant heterogeneity among the CFU data for each infected animal, in terms of the magnitude and the timing of the response (Figure 2A and Table S3). One infected animal (TI3 - which had the highest CFU/ml data) peaked at 24hpi, two others (TI1 and TI4) peaked at 36hpi and CFU data for one animal was still climbing at 48hpi (TI5). Additionally, one infected animal was observed to have only a very modest increase in bacterial counts (TI2). Somatic cell count (SCC) data also confirmed the presence of the infection in the challenged animals and not in the controls. SCC was observed to increase at 24hpi and by 36hpi was, on average, >900,000 cells/ml in infected animals. In comparison, the average SCC in control animals at 36hpi was <52,000 cells/ml (Figure 2B & Table S3). An SCC reading >200,000 cells/ml is generally considered diagnostic of mastitis (Dufour & Dohoo, 2013). Again there was heterogeneity in the SCC response in the infected

animals. Interestingly, the infected animal that was observed to have only a modest increase in CFU/ml (TI2) had a relatively robust SCC response.

Profiling mRNA Expression in Blood and Milk Isolated CD14+ Monocytes

A next generation sequencing approach was applied to monitor the transcriptional (mRNAseq) and post-transcriptional (miRNAseq) changes that occurred in both blood and milk isolated CD14+ monocytes in the infected and control animals (Figure 1). Sequencing of 100 mRNA Illumina libraries (i.e. 50 blood and 50 milk monocyte mRNA libraries) yielded >4 billion sequence reads. More than 3 billion reads of these mapped uniquely to the *Bos taurus* UMD 3.1 genome (Table S2). The average correlation coefficient of mRNA normalised read counts between samples at each time-point was 0.95 for control samples and 0.92 for infected samples indicating very high reproducibility of the data among replicates (Table S4).

Hierarchical Clustering of normalised mRNA read counts from MIMs revealed that the control and infected animals clearly separated at 36 and 48hpi except for the one infected sample (TI2) which had very low bacterial counts and likely did not developed a full infection (Figure 2C-F). This sample was subsequently excluded from differential gene expression analysis. Hierarchical Clustering of the normalised mRNA read counts of genes that were differentially expressed in blood isolated monocytes (BIMs) revealed that only 3 of the infected animals (TI1, TI3 and TI4) separated from uninfected controls at 36 and 48hpi (Figure S1). These animals also had the highest SCC data at these time-points.

We utilised the EdgeR statistical package (Robinson *et al.*, 2010) to determine which mRNAs were significantly differentially expressed in MIMs and BIMs in

response to *S. uberis*. In MIMs, there were 4, 36, 1774, and 1532 up-regulated genes at 12, 24, 36 and 48hpi, respectively. The majority (1,254) of genes up-regulated at 48hpi were also up-regulated at 36hpi. Additionally, there were 5, 2, 1518 and 995 down-regulated genes in MIMs at those time-points. Of the 995 down-regulated genes at 48hpi, 80% were also down-regulated at 36hpi. Overall, 2056 different genes were up-regulated and 1721 different genes were down-regulated for at least one time-point in MIMs in response to *S. uberis* infection (Table S5).

Traditionally, mastitis has been thought of as a local bacterial infection with a robust inflammatory response. In BIMs, however, we observed a much more subtle but still quite significant response to *S. uberis* infection. Only, ten genes were up-regulated in BIMs at 36hpi but this increased to 83 genes by 48hpi (Table S5). Nine of the ten 36hpi genes were also up-regulated at 48hpi. Additionally, 3, 4, 26, and 39 genes were down-regulated in BIMs at 12, 24, 36 and 48hpi, respectively.

Pathway Analysis Reveals the Suppression of Metabolic Pathways and the Up-regulation of Inflammatory Pathways in Response to S. uberis Infection

Pathway analysis of up- and down-regulated genes at each time-point was undertaken using GOseq (Young *et al.*, 2010) with pathway annotation imported from the KEGG database (Kanehisa *et al.*, 2007) to identify which pathways were statistically overrepresented among DE genes in MIMs and BIMs. Two manually curated pathways (Interferon signalling pathway and the Inflammasome pathway) were also included (see methods). No significant pathways were identified among either the BIM or MIM DE genes at 12 or 24hpi. At 36 and 48hpi, however, more than 20 different pathways were identified as being statistically overrepresented (Figure 3 and

Table S6). In MIMs, down-regulated genes were predominantly associated with metabolic pathways (Figure S2), such as fatty acid and amino acid metabolism, the citric acid (TCA) cycle and glutathione metabolism, as well as DNA replication and repair pathways and the cell cycle. Down-regulated pathways were largely similar between 36hpi and 48hpi, though fewer pathways were significant at 48hpi. Up-regulated genes, on the other hand, were primarily associated with well-known pattern recognition receptor (PRR) pathways (Figure 4) including the *Toll-like receptor pathway* (e.g. TLR2, TLR4, CD14, MYD88, TIRAP, and IRAK1 all up-regulated), the *NOD-like receptor pathway* (e.g. NOD1, NOD2, NLRP3 (NALP3), NLRC4 (IPAF), NAIP (NAIP5) up-regulated) and the *RIG-I-like receptor pathway* (e.g. DDX58 (RIG-I), IFIH1 (MDA5), CYLD, DHX58 (LGP2), DDX3X, TRIM25); *interferon signalling* and *cytokine and chemokine signalling* pathways. Up-regulated inflammatory cytokine and chemokine genes included the genes encoding TNF, IL1A, IL1B, IL6, IL8, IL12A and IL12B, IL17B and IL17C, IL18, IL23A, IL27, CCL3 (MIP1α) CCL4 (MIP1β), CCL5 (RANTES), CCL8 (MCP-2) and CCL20 (MIP3A). The genes encoding TNF, IL1B, IL6, IL12 and CCL20 were more than 10 fold up-regulated at 36hpi. All up-regulated pathways that were significant at 36hpi were still significant at 48hpi, with 5 additional up-regulated pathways being significant only at 48hpi. These pathways were primarily related to leukocyte migration and phagocytosis.

In BIMs, only two pathways were statistically over-represented among 48hpi up-regulated genes - *Interferon signalling* and *Cytokine-cytokine receptor interaction* (Table S6). No pathways were significant at the other time-points. Among down-regulated genes, there were also few over-represented pathways. Those pathways that

were significant were primarily related to the complement and focal adhesion pathways.

Network Analysis of Differentially Expressed Genes

InnateDB was used to generate a network of experimentally-supported molecular interactions that have been annotated to occur directly between the differentially expressed genes and their encoded products. Gene expression data from each of the four post-infection time-points was then overlaid on this network and the network was visualised using Cytoscape 2.8.2 (Shannon *et al.*, 2003) (Figure 2 G-J). The network consisted of 2,185 nodes (representing differentially expressed genes and their encoded products) and 10,786 edges (representing annotated molecular interactions) between them.

The network was then analysed using cytoHubba (Lin *et al.*, 2008) to identify network hubs and bottlenecks which may represent the key regulatory nodes in the networks. Using the "Degree" algorithm the top 20 hubs (i.e. genes/proteins that are highly connected to other DE genes) in each network were identified (Table S7). InnateDB Gene Ontology analysis revealed that the top 20 hubs were highly enriched for roles in innate immunity (FDR < $1.7e^{-8}$) and transcriptional regulation (FDR < $1.5e^{-7}$). Indeed, many of the top 20 hubs were well-known transcriptional regulators of innate immunity including JUN, NFKB1, RELA, STAT1, STAT3, EP300, and CREBBP. These transcriptional regulators were located in the most densely connected portion of the network and share many connections (Figure 5A). One interpretation of this is that transcriptional regulation by several of these transcription factors is required for differential gene expression in response to the infection.

Bottlenecks are network nodes that are the key connector proteins in a network and have many “shortest paths” going through them, similar to bridges or tunnels on a highway map (Yu *et al.*, 2007). 17 of the top 20 hubs were also identified as network bottlenecks. Beta-actin (ACTB), the transcriptional regulator, FOS (AP1), and ISG15, were additionally identified in the top 20 bottlenecks. ISG15 has been shown to act as a negative regulator of both the NFκB and RIG-I signalling pathways (Arnaud *et al.*, 2011; Minakawa *et al.*, 2008)

Identifying hubs solely based on their degree can identify nodes that, in general, have been annotated to have lots of interactions. This fails to address whether the number of connections in a particular network of interest is more or less than is expected (given the number of known interactions for that node in the database and the size of the network). To address this issue, we have developed the Contextual Hub Analysis Tool (CHAT) (Wiencko *et al*., unpublished), a network analysis tool which identifies nodes in a network that are more highly connected to contextually relevant nodes (in this case differentially expressed nodes) than is expected by chance (Table S8). Applying this method to our network identified that several of the hub nodes (e.g. KIAA0101), did not have more connections to differentially expressed genes than expected by chance. This means that these genes, although highly connected, are less likely to be functionally important in our network. On the other hand, all of the transcriptional regulators of innate immunity that were identified as hubs in the analysis above (JUN, NFKB1, RELA, STAT1, STAT3, EP300, CREBBP), were also identified by CHAT to be significantly more connected to 36hpi differentially expressed genes than expected by chance. CHAT also identified several other known innate immunity transcriptional regulators in the top 20 "contextual" hubs including REL, IRF1, and IRF9. Indeed 15 of the top 20 contextual hubs are annotated by

InnateDB as having a role in innate immunity (FDR < $1.16E^{-12}$). Although the ranking of the top contextual hubs changed from 36 to 48hpi, the most significant hubs remained the same.

The network was also analysed using the jActiveModules plugin (Ideker *et al.*, 2002) in Cytoscape 2.8.2 (Shannon *et al.*, 2003) to identify high-scoring differentially expressed sub-networks. This type of analysis can aid in the identification of functionally relevant groups of differentially expressed genes that may be acting in concert. A single highly connected component (>10 nodes) was identified consisting of 278 nodes and 1,585 interactions. This module consisted of several of the transcriptional hubs (CREBBP, EGR1, EP300, NFKB1, RELA) identified in the analysis above and their interactors (Figure 5B). Pathway analysis of genes in the module revealed that the module was statistically enriched for many of the same pathways that were identified in the analysis of all up-regulated genes including Jak-STAT signalling, the TLR, NLR and RIG-I pathways, apoptosis, and chemokine and cytokine signalling (Table S9).

Profiling miRNA Expression in Blood and Milk Isolated CD14+ Monocytes

Sequencing of 100 miRNA Illumina libraries yielded over 1 billion reads for both the MIM and BIM samples. Following a pipeline of quality filtering and adaptor trimming, a total of 312 and 492 million reads from MIMs and BIMs, respectively, mapped uniquely to the *Bos taurus* UMD 3.1 genome (Table S2). Uniquely aligning reads were then assigned to known mRNAs/miRNAs using HTseq based on miRBase v19 annotation of the bovine genome to generate read counts per mature miRNA in

each sample (Flicek *et al.*, 2012; Hubbard *et al.*, 2009). On average, 79% of MIM reads and 80% of BIM reads, uniquely mapped to known miRNAs (Figure S3).

RNAseq profiling revealed that the miRNAome of MIMs and BIMs were broadly similar and exhibited a range of miRNA expression that has been observed in many other cell-types. 297 and 282 miRNAs were expressed at a threshold of >1 rpm in MIMs and BIMs, respectively (Table S10). Of these, 136 and 116, respectively, were expressed at a level >100 rpm, a level of expression that has been shown to be associated with functional miRNAs (Mullokandov *et al.*, 2012).

Multiple miRNAs are Differentially Expressed in Response to S. uberis Infection

The EdgeR statistical package was utilised to determine which miRNAs were significantly differentially expressed in response to *S. uberis* infection at 12, 24, 36, and 48hpi. To address any normalisation issues we retained only those miRNAs that were robust to the normalisation procedure used (Lawless *et al.*, 2013). Additionally, only miRNAs that had an average expression of >10 rpm across samples were included for further analysis. In MIMs, we identified that 26 unique miRNAs were differentially expressed. Twelve of these miRNAs were differentially expressed across more than one time-point (Table 1). Hierarchical clustering of the normalised read counts for MIM differentially expressed miRNAs revealed that the control and infected animals clearly separated at 36hpi (Figure 6). Very few miRNAs were differentially expressed in blood monocytes. We found 3 in total, 1 at 24hpi and 3 at 48hpi (1 was differentially expressed at both time-points) (Table 1).

Many of the miRNAs identified as being differentially expressed have been shown to have a role in immunity in other species. miR-223, for example, which was

up-regulated at 36hpi in MIMs, has a multi-factorial role in neutrophils, regulating their proliferation, activation and granulopoiesis (Chen *et al.*, 2004; Fazi *et al.*, 2005). Interestingly, in RAW264.7 cells challenged with LPS, miR-223 has been reported to be down-regulated, allowing the up-regulation of signal transducer and activator of transcription 3 (STAT3), which promotes pro-inflammatory IL-6 and IL-1β transcription. We have previously commented on the differences in the miRNA response to LPS and *S. uberis*, a Gram-positive bacterium (Lawless *et al.*, 2013).

Other DE miRNAs in our study that have a demonstrated role in immunity and infection in other species includes let-7e, which was down-regulated in MIMs following *S. uberis* infection. Let-7e, has been shown to regulate Caspase 3 and 7 in human monocyte derived macrophages infected with *Mycobacterium avium hominissuis* (Sharbati *et al.*, 2011). Let-7e, as well as several other DE miRNAs in our study (bta-miR-200c, bta-miR-210, and bta-miR-193a) have also previously been identified as DE in bovine mammary epithelial cells stimulated with *S. uberis in vitro* (Lawless *et al.*, 2013).

Another DE miRNA with a role in immune regulation is miR-150, which we observed to be down-regulated at both 36 and 48hpi in MIMs. miR-150 targets MyD88 (up-regulated at both 36 and 48hpi in MIMs), a key regulator of TLR signalling (Ghorpade *et al.*, 2013). miR-150 has also been shown to target CXCR4 (Rolland-Turner *et al.*, 2013; Tano *et al.*, 2011), which was up-regulated 2-fold at 36 and 48hpi in MIMs. Finally, one of the miRNAs that was identified as down-regulated in BIMs, miR-146b, has been shown to target TNF receptor-associated factor 6 (TRAF6) and IL-1 receptor-associated kinase 1 (IRAK1) genes in THP-1 cells stimulated with LPS (Taganov *et al.*, 2006).

The Predicted Targets of Down-regulated but not Up-regulated miRNAs are Highly Enriched for Roles in Innate Immunity

To identify the potential mRNA targets of differentially expressed miRNAs in MIMs isolated from infected animals we identified those mRNAs whose expression was significantly negatively correlated with miRNA expression. These predictions were further refined by removing those miRNA-target predicted relationships that were not supported by a predicted seed region in the 3' UTR of the correlated mRNA (Figure 7, Table S11). Analysis of the predicted target genes using InnateDB (www.innatedb.com) (Lynn *et al.*, 2008), revealed that the predicted targets of down-regulated but not up-regulated miRNAs were highly enriched for roles in innate immunity (FDR < $3.2E^{-8}$). More specifically, pathway analysis revealed that down-regulated miRNAs were predicted to preferentially target key pathogen recognition receptor (PRR) signalling pathways including the TLR, NLR and RIG-I signalling pathways (Table S12). Given that these pathways were also identified in the mRNAseq data as being among the top up-regulated pathways, this finding strongly suggests that miRNAs are key regulators of innate immune pathways which drive the host inflammatory response during mastitis.

In contrast, the predicted targets of up-regulated miRNAs were enriched for roles in metabolism (FDR = 0.01). Pathway analysis of the mRNAseq data had already highlighted the down-regulation of metabolic pathways in response to *S. uberis* infection (see above). These results suggest that miRNAs may also be key regulators of the transcriptional suppression of metabolic pathways during mastitis.

Novel miRNA discovery

The miRNA sequencing data was also mined to determine if milk or blood monocytes expressed potentially novel miRNAs. Previously, we identified 19 novel miRNAs in bovine mammary epithelial cells using miRDeep2 (Lawless *et al.*, 2013). Applying the same approach as our previous study we identified a further 20 high-confidence putatively novel bovine miRNAs that were independently predicted in multiple MIMs/BIMs miRNAseq data (Table S13).

Searching the miRBase database (v 20) using BLAST identified that 8 of the novel miRNAs had close homology to other miR-2284 family members. miRBase currently lists this miRNA family as having 102 members, yet virtually no data exists regarding what function such a large group of constitutively expressed miRNAs may have. Other novel miRNAs discovered in this study included a homolog of hsa-miR-3680-3p, a miRNA identified in human periphery blood (Vaz *et al.*, 2010). The discovery of these miRNA further adds to the database of bovine miRNAs.

DISCUSSION

Infectious disease is a serious threat not only directly to human health but also to animal health, where it is associated with substantial annual economic losses, public confidence issues and food security concerns. Currently, there is a significant gap in the understanding of the molecular and genetic mechanisms which underpin susceptibility to infectious disease both in humans and in animals. An important reason for this is the fact that disease susceptibility is a multi-factorial complex phenotype, which is not the result of single genes acting in isolation but rather is due to perturbation at a network or systems level (Barabasi *et al.*, 2011). Such networks are regulated at multiple different levels (e.g. genetic, transcriptional, post-transcriptional) and as such a multi-omic integrative biology approach is needed to understand them.

Here, we report a next generation sequencing approach coupled with advanced network and pathway biology methods to simultaneously profile the mRNA and miRNA networks that are differentially regulated *in vivo* in blood and milk isolated CD14+ monocytes during infection with a bovine mastitis pathogen, *S. uberis*. Bovine mastitis is an inflammation-driven disease of the bovine mammary gland, which costs the global dairy industry billions of dollars per annum (Jones, 2009; Wells *et al.*, 1998). Profiling genome-wide changes in mRNA expression in MIMs and BIMs using RNAseq, we observed more than 3,500 genes to be statistically altered in their expression in response to *S. uberis* challenge. Notably, this RNAseq approach identified approximately 1,000 more differentially expressed genes than had been previously reported in a microarray based analysis of RNA expression in mammary tissue of cattle infected with the same pathogen (Jensen *et al.*, 2013; Moyes *et al.*,

2009; Swanson *et al.*, 2009). As expected, given that mastitis is a relatively localised inflammatory disease in the mammary gland, the majority of differentially expressed genes were identified in MIMs, which are recruited to the site of infection. This influx of immune cells (including monocytes) to the site of infection was observed in recorded SCC data only in the infected animals. We also, however, observed a small but significant transcriptional response in BIMs to *S. uberis* infection that was primarily associated with an interferon and cytokine signalling signature. Previous studies have also shown more systemic changes in gene expression in neighbouring uninfected mammary glands, the liver and in the blood (Blum *et al.*, 2000; Jensen *et al.*, 2013; Jiang *et al.*, 2008; Mitterhuemer *et al.*, 2010).

The predominant signature associated with up-regulated mRNAs in MIMs from *S. uberis* infected animals was the strong transcriptional activation of innate immune and inflammatory gene expression. In particular, we noted the transcriptional activation of key pattern recognition pathways including the TLR, NLR and RIG-I pathways, which likely drive the observed pro-inflammatory response. The involvement of TLR signalling (particularly TLR 2 and 4) in the host response to mastitis is well documented (Buitenhuis *et al.*, 2011; Ma *et al.*, 2011; Mitterhuemer *et al.*, 2010; Porcherie *et al.*, 2012; Whelehan *et al.*, 2011), however, less is known about the involvement of the NLR and RIG-I pathways (Moyes *et al.*, 2009). Interestingly, the RIG-I pathway is classically associated with viral RNA recognition, however, recent findings suggest that RIG-I can also recognise nucleic acids released by invasive bacteria and trigger IFN-β and inflammasome activation (Abdullah *et al.*, 2012). These findings concur well with the observed interferon and inflammasome activation transcriptional signatures observed in our study.

Several previous *in vitro* studies have strongly suggested roles for miRNAs in regulating bovine immunity (Dilda *et al.*, 2011; Lawless *et al.*, 2013), however none of these have globally profiled the miRNA response to infection *in vivo*. In this study, we have also used next generation sequencing to profile miRNA expression in MIMs and BIMs following *S. uberis* infection. 26 miRNAs were identified as DE in MIMs and 3 were identified in BIMs. Several of these have been previously described as targeting immune or inflammatory regulators in other species. Of particular interest is our finding that down-regulated but not up-regulated miRNAs in MIMs are predicted to preferentially target genes involved in innate immunity and inflammation. Furthermore, the TLR, NLR and RIG-I pathways discussed above were all preferentially predicted to be targeted. This strongly suggests that the transcriptional suppression of these miRNAs enables the activation and amplification of the pro-inflammatory response. Further supporting this conclusion is the fact that several of the DE miRNAs in our study have been validated to target genes in these pathways in other species. miR-149, for example, which was down-regulated in MIMs following *S. uberis* infection, has been shown to target mouse CD14 and IRAK1 (Chi *et al.*, 2009), key signalling proteins in the TLR pathway. Both CD14 and IRAK1 are also predicted to be targets of bta-miR-149 in our study.

The other predominant transcriptional signature that we found in MIMs following *S. uberis* infection was the wide-spread repression of a number of metabolic processes (> 150 KEGG-annotated metabolism genes are down-regulated at 36hpi). Interestingly, we found that up-regulated miRNAs were predicted to preferentially target genes involved in metabolism, suggesting that miRNAs, which are up-regulated in response to *S. uberis* infection may contribute to the transcriptional suppression of metabolic pathways. This signature of metabolic gene transcriptional suppression may

appear initially paradoxical in light of the fact that production of inflammatory cytokines is expected to require substantial energy consumption. Indeed, it is now becoming widely appreciated that activated macrophages undergo the Warburg effect, switching their metabolism from oxidative phosphorylation to glycolysis (McGettrick & O'Neill, 2013). This metabolic switch has recently been investigated using a combined metabolomics and microarray approach (Tannahill *et al.*, 2013) and has revealed the up-regulation of a number of genes involved in glycolysis in bone-marrow derived macrophages (BMDMs) challenged with lipopolysaccharide (LPS) (e.g. solute carrier family 2 (facilitated glucose transporter), member 1 (*SLC2A1/GLUT1*), hexokinase 3 (*HK3*), fructose-2,6-biphosphatase 3 (*PFKFB3*)) and the down-regulation of several key genes encoding enzymes in the TCA cycle (e.g. malate dehydrogenase 1 (*MDH1*) and isocitrate dehydrogenase 2 (*IDH2*)). Our transcriptional data is very consistent with the data presented in this paper (e.g. *SLC2A1*; *HK2* and *HK3* and *PFKFB4* are all up-regulated and *MDH1* and *IDH1* are down-regulated in MIMs at 36hpi) and suggests that although there is a broad signature of transcriptional suppression of metabolism, these cells are likely to be highly glycolytically active. Several other genes encoding enzymes in the TCA cycle (which was statistically over-represented among down-regulated genes) were also transcriptionally repressed in MIMs at 36hpi including dihydrolipoamide dehydrogenase (DLD); fumarate hydratase (FH); IDH3B; pyruvate dehydrogenase beta (PDHB); MDH2; succinate dehydrogenase complex, subunit B (SDHB); succinate-CoA ligase, alpha subunit (SUCLG1). As has also recently been shown in BMDMs, LPS strongly increases levels of succinate, a TCA cycle intermediate (Tannahill *et al.*, 2013). Succinate acts as an inflammatory signal in macrophages inducing *IL1B* through the transcription factor HIF1α, both of which are

transcriptionally activated in MIMs 36hpi (*IL1B* is 10 fold up-regulated). Another metabolic pathway that is significantly transcriptionally repressed in MIMs at 36 and 48hpi is the KEGG *Valine, leucine and isoleucine degradation* pathway. Valine, leucine and isoleucine are branch-chain amino acids which are converted into Acyl-CoA derivatives. These are converted either into acetyl-CoA or succinyl-CoA and enter the TCA cycle (Sears *et al.*, 2009). Most of the other significantly down-regulated pathways including *Fatty acid metabolism; Propanoate metabolism; Butanoate metabolism; Tryptophan metabolism; beta-Alanine metabolism; Lysine degradation and Glyoxylate and dicarboxylate metabolism*; also result in the production of acetyl-CoA and succinyl-CoA that enter the TCA cycle. A similar pattern of expression leading to the transcriptional down-regulation of the TCA cycle and alternative pathways involved in producing TCA cycle components has also been reported in other infection models (Chin *et al.*, 2010). The transcriptional repression of these pathways is therefore also consistent with a switch in metabolism from oxidative phosphorylation to glycolysis during the pro-inflammatory response.

Another pathway that is significantly down-regulated is the KEGG *primary bile acid biosynthesis* pathway. Despite the potentially misleading name, this pathway primarily consists of the reactions involved in cholesterol metabolism. The down-regulation of genes involved in cholesterol metabolism has also been reported in monocytes isolated from HIV+ individuals (Feeney *et al.*, 2013) and a number of bacterial infections (Dushkin, 2012). The accumulation of cholesterol in monocytes and macrophages leads to the formation of foam cells, which in humans are associated with the inflammatory disease, atherosclerosis (Ross, 1999). The down-regulation of genes involved in cholesterol and fatty acid metabolism is likely driven in part by the transcriptional suppression of the PPAR-γ transcription factor in MIMs at 36hpi and

the down-regulation of PPAR-α at 48hpi, both of which are key transcriptional regulators of these pathways (Dushkin, 2012). Interestingly, the PPARs also have a role in the regulation of inflammation, where their suppression is required to induce inflammatory gene expression (Bensinger & Tontonoz, 2008). Of further note is that one of the liver X receptors, LXR-β (NR1H2), which together with the PPARs is a key regulator of inflammation and lipid metabolism (Bensinger & Tontonoz, 2008), is up-regulated in MIMs at 36 and 48hpi. LXRs are also known to antagonise inflammatory gene expression, so it is somewhat surprising to find LXR-β to be up-regulated. This may reflect the fact that balance is needed to avoid excessive inflammation or that LXRs and PPARs do not completely overlap in the genes that they regulate.

An additional link between metabolism and inflammation that is currently under intensive investigation is the role of NAD+, sirtuins (SIRTs) and AMP-dependent protein kinase (AMPK) in suppressing inflammation (McGettrick & O'Neill, 2013). The activation of TLR4, which along with TLR2 and TLR9 is transcriptionally up-regulated in MIMs at 36hpi, has been shown to induce NAM phosphoribosyltransferase (NAMPT; up-regulated in MIMs at 36hpi), which in turn activates SIRT1 (up-regulated in MIMs at 36hpi) via NAD+. SIRT1 limits inflammation by repressing RELA transcription factor activity, a key transcriptional hub identified in MIMs. SIRT1 also activates AMPK (up-regulated in MIMs at 36hpi), a central regulator of energy metabolism. Activation of AMPK has been shown to decrease NFκB activity and TNFα production in macrophages stimulated with LPS; IL12 production in DCs; and HIF1α. This data suggests that at 36hpi, the brakes are starting to be applied to limit the inflammatory response to *S. uberis* infection via SIRT1 and AMPK. The affect of this break is apparent at 48hpi where

the genes encoding TNFα, IL1B, IL12 and HIF1α are all down-regulated in comparison to 36hpi. The limiting of inflammation at this stage makes sense based on the bacterial count data, which shows that bacterial CFU/ml are dropping, suggesting that the infection is being resolved. Interestingly, AMPK activity also inhibits both the cholesterol and fatty acid metabolic pathways that, as discussed above, are down-regulated in MIMs following *S. uberis* infection. This suppression of fatty acid metabolism has been shown to be beneficial to the host during a viral infection (Moser *et al.*, 2012).

Finally, we also observed the statistically significant over-representation of down-regulated genes annotated in the KEGG *glutathione metabolism* pathway. Glutathione has an important role in innate and adaptive immunity and has been shown to confer protection against microbial, viral and parasitic infections (Morris *et al.*, 2013). Glutathione metabolism also plays an important role in macrophages in the detoxification of reactive oxygen species (ROS). The transcriptional suppression of this pathway in MIMs following *S. uberis* infection may be a consequence of the metabolic switch to glycolysis and may be detrimental to the host leading to an excess of oxidants in the cells, which could drive the inflammation and tissue damage that are characteristic of mastitis. Indeed, in patients with active tuberculosis, PBMC intracellular glutathione levels dropped by 70%, this was correlated with increased pro-inflammatory cytokines and enhanced bacterial growth (Guerra *et al.*, 2012). Supplementation with glutathione has been demonstrated to lead to the control of mycobacterial growth (Venketaraman *et al.*, 2003) and also appears to have beneficial effects in reducing inflammation in HIV+ patients (Morris *et al.*, 2012). This suggests that glutathione supplementation is a potential strategy to reduce the effects of inflammation in mastitis.

miRNAs also likely play a key role in regulating the links between inflammation and metabolism observed in this study. Human SIRT1, for example, which as discussed above limits inflammation, has been shown to be a target of miR-34a (Yamakuchi *et al.*, 2008). Our data is consistent with this relationship also existing in MIMs, where we have found bta-miR-34a to be down-regulated at 36 and 48hpi and SIRT1 up-regulated. Other examples of miRNAs that likely transcriptionally regulate metabolic pathways in MIMs include miR-451, which is up-regulated in MIMs at 36 and 48hpi, and has been shown to target MO25 in mouse heart tissue altering AMPK signalling (Chen *et al.*, 2012). miR-451 has also been shown to regulate the expression of several pro-inflammatory cytokines in mice in response to influenza infection (Rosenberger *et al.*, 2012).

Aside from providing new insight into the regulatory role miRNAs play in *S. uberis* infection *in vivo*, our study also provides the ground-work for a number of potential practical applications in veterinary medicine. miRNAs, for example, exhibit many properties that have made them of significant interest as non-invasive biomarkers. miRNAs are abundantly and stably expressed in a range of accessible tissues including serum, milk, urine, saliva and semen where they can be readily measured (Chen *et al.*, 2010; Hata *et al.*, 2010; Kosaka *et al.*, 2010). Importantly for a potential biomarker, miRNAs have a high information content, and the expression profile of small numbers of them have been shown to be diagnostic of disease (De Guire *et al.*, 2013). The use of miRNAs as a clinical biomarker is most advanced in human cancer research. In 2009, Prometheus Laboratories released a miRNA biomarker to accurately identify 25 different tumour types (Ajit, 2012), and miRNA biomarkers are now available for early cancer prognosis from two further companies Asuragen & Rosetta Genomics. Next generation sequencing based technologies, such

as the approach used in this study, are empowering RNA expression profiling, including miRNAs, on a genome-wide scale with unprecedented resolution, accuracy and speed and at a relatively low cost (Schuster, 2008). There is significant potential to develop these approaches as diagnostics of infection in animals but also in humans too.

Acknowledgements

We would also like to thank the excellent technical help of Randy Atchison, Derrel Hoy, Tera Nyholm, Adrienne Staple, Jen Jones, and Paul Amundson. We would also like to thank Prof Luke O'Neill for his correspondence. This study was funded in part by Teagasc RMIS 6018 and United States Department of Agriculture ARS funding 3625-32000-102-00. NL is supported by a Teagasc Walsh Fellowship.

Author Contributions

Conceived and designed the experiments: NL, TAR, JDL, DJL. Performed the experiments: NL, BP, DZ, JDL. Library preparation and sequencing: MB. Analyzed and interpreted the data: NL, KB, COF, DJL. Wrote the paper: NL, DJL with input from COF, TS, TAR, KZ, JDL. All authors reviewed the final draft of the paper.

Conflict of Interests

The authors have declared that no conflicting interests exist.

REFERENCES

Abdullah, Z., Schlee, M., Roth, S., Mraheil, M. A., Barchet, W., Bottcher, J., *et al.* (2012). RIG-I detects infection with live Listeria by sensing secreted bacterial nucleic acids. *The EMBO journal* **31,** 4153-64.

Ajit, S. K. (2012). Circulating microRNAs as Biomarkers, Therapeutic Targets, and Signaling Molecules. *Sensors* **12,** 3359-69.

Arnaud, N., Dabo, S., Akazawa, D., Fukasawa, M., Shinkai-Ouchi, F., Hugon, J., *et al.* (2011). Hepatitis C virus reveals a novel early control in acute immune response. *PLoS pathogens* **7,** e1002289.

Auer, P. L.Doerge, R. W. (2010). Statistical design and analysis of RNA sequencing data. *Genetics* **185,** 405-16.

Bannerman, D. D., Paape, M. J., Goff, J. P., Kimura, K., Lippolis, J. D. &Hope, J. C. (2004). Innate immune response to intramammary infection with Serratia marcescens and Streptococcus uberis. *Vet Res* **35,** 681-700.

Barabasi, A. L., Gulbahce, N. &Loscalzo, J. (2011). Network medicine: a network-based approach to human disease. *Nature reviews. Genetics* **12,** 56-68.

Benjamini, Y.Hochberg, Y. (1995). Controlling the False Discovery Rate: A Practical and Powerful Approach to Multiple Testing. *J. R. Stat. Soc. Ser. B Stat. Methodol.* **57,** 289-300.

Bensinger, S. J.Tontonoz, P. (2008). Integration of metabolism and inflammation by lipid-activated nuclear receptors. *Nature* **454,** 470-7.

Blum, J. W., Dosogne, H., Hoeben, D., Vangroenweghe, F., Hammon, H. M., Bruckmaier, R. M., *et al.* (2000). Tumor necrosis factor-alpha and nitrite/nitrate responses during acute mastitis induced by Escherichia coli infection and endotoxin in dairy cows. *Domestic Animal Endocrinology* **19,** 223-35.

Bronevetsky, Y., Villarino, A. V., Eisley, C. J., Barbeau, R., Barczak, A. J., Heinz, G. A., *et al.* (2013). T cell activation induces proteasomal degradation of Argonaute and rapid remodeling of the microRNA repertoire. *The Journal of experimental medicine* **210,** 417-32.

Buitenhuis, B., Rontved, C. M., Edwards, S. M., Ingvartsen, K. L. &Sorensen, P. (2011). In depth analysis of genes and pathways of the mammary gland involved in the pathogenesis of bovine Escherichia coli-mastitis. *BMC Genomics* **12,** 130.

Bullard, J. H., Purdom, E., Hansen, K. D. &Dudoit, S. (2010). Evaluation of statistical methods for normalization and differential expression in mRNA-Seq experiments. *BMC bioinformatics* **11,** 94.

Chen, C. Z., Li, L., Lodish, H. F. &Bartel, D. P. (2004). MicroRNAs modulate hematopoietic lineage differentiation. *Science* **303,** 83-6.

Chen, H., Untiveros, G. M., McKee, L. A., Perez, J., Li, J., Antin, P. B., *et al.* (2012). Micro-RNA-195 and -451 regulate the LKB1/AMPK signaling axis by targeting MO25. *PloS one* **7,** e41574.

Chen, X., Gao, C., Li, H., Huang, L., Sun, Q., Dong, Y., *et al.* (2010). Identification and characterization of microRNAs in raw milk during different periods of lactation, commercial fluid, and powdered milk products. *Cell research* **20,** 1128-37.

Chi, S. W., Zang, J. B., Mele, A. &Darnell, R. B. (2009). Argonaute HITS-CLIP decodes microRNA-mRNA interaction maps. *Nature* **460,** 479-86.

Chin, C. Y., Monack, D. M. &Nathan, S. (2010). Genome wide transcriptome profiling of a murine acute melioidosis model reveals new insights into how Burkholderia pseudomallei overcomes host innate immunity. *BMC Genomics* **11,** 672.

Cock, P. J., Fields, C. J., Goto, N., Heuer, M. L. &Rice, P. M. (2010). The Sanger FASTQ file format for sequences with quality scores, and the Solexa/Illumina FASTQ variants. *Nucleic acids research* **38,** 1767-71.

Coutinho, L. L., Matukumalli, L. K., Sonstegard, T. S., Van Tassell, C. P., Gasbarre, L. C., Capuco, A. V., *et al.* (2007). Discovery and profiling of bovine microRNAs from immune-related and embryonic tissues. *Physiological genomics* **29,** 35-43.

De Guire, V., Robitaille, R., Tetreault, N., Guerin, R., Menard, C., Bambace, N., *et al.* (2013). Circulating miRNAs as sensitive and specific biomarkers for the diagnosis and monitoring of human diseases: promises and challenges. *Clinical Biochemistry* **46,** 846-60.

Dilda, F., Gioia, G., Pisani, L., Restelli, L., Lecchi, C., Albonico, F., *et al.* (2011). Escherichia coli lipopolysaccharides and Staphylococcus aureus enterotoxin B differentially modulate inflammatory microRNAs in bovine monocytes. *Veterinary journal* **192,** 514-516.

Dong, C., Zhao, G., Zhong, M., Yue, Y., Wu, L. &Xiong, S. (2013). RNA sequencing and transcriptomal analysis of human monocyte to macrophage differentiation. *Gene* **519,** 279-87.

Dufour, S.Dohoo, I. R. (2013). Monitoring herd incidence of intramammary infection in lactating cows using repeated longitudinal somatic cell count measurements. *Journal of Dairy Science* **96,** 1568-80.

Dushkin, M. I. (2012). Macrophage/foam cell is an attribute of inflammation: mechanisms of formation and functional role. *Biochemistry. Biokhimiia* **77,** 327-38.

Fazi, F., Rosa, A., Fatica, A., Gelmetti, V., De Marchis, M. L., Nervi, C., *et al.* (2005). A minicircuitry comprised of microRNA-223 and transcription factors NFI-A and C/EBPalpha regulates human granulopoiesis. *Cell* **123,** 819-31.

Feeney, E. R., McAuley, N., O'Halloran, J. A., Rock, C., Low, J., Satchell, C. S., *et al.* (2013). The expression of cholesterol metabolism genes in monocytes from HIV-infected subjects suggests intracellular cholesterol accumulation. *The Journal of infectious diseases* **207,** 628-37.

Flicek, P., Amode, M. R., Barrell, D., Beal, K., Brent, S., Carvalho-Silva, D., *et al.* (2012). Ensembl 2012. *Nucleic acids research* **40,** D84-90.

Garmire, L. X.Subramaniam, S. (2012). Evaluation of normalization methods in mammalian microRNA-Seq data. *RNA* **18,** 1279-88.

Ghorpade, D. S., Holla, S., Kaveri, S. V., Bayry, J., Patil, S. A. &Balaji, K. N. (2013). Sonic hedgehog-dependent induction of microRNA 31 and microRNA 150 regulates Mycobacterium bovis BCG-driven toll-like receptor 2 signaling. *Molecular and Cellular Biology* **33,** 543-56.

Guerra, C., Johal, K., Morris, D., Moreno, S., Alvarado, O., Gray, D., *et al.* (2012). Control of Mycobacterium tuberculosis growth by activated natural killer cells. *Clinical and Experimental Immunology* **168,** 142-52.

Hata, T., Murakami, K., Nakatani, H., Yamamoto, Y., Matsuda, T. &Aoki, N. (2010). Isolation of bovine milk-derived microvesicles carrying mRNAs and

microRNAs. *Biochemical and biophysical research communications* **396,** 528-33.

Hubbard, T. J., Aken, B. L., Ayling, S., Ballester, B., Beal, K., Bragin, E., *et al.* (2009). Ensembl 2009. *Nucleic acids research* **37,** D690-7.

Ideker, T., Ozier, O., Schwikowski, B. &Siegel, A. F. (2002). Discovering regulatory and signalling circuits in molecular interaction networks. *Bioinformatics* **18 Suppl 1,** S233-40.

Jensen, K., Gunther, J., Talbot, R., Petzl, W., Zerbe, H., Schuberth, H. J., *et al.* (2013). Escherichia coli- and Staphylococcus aureus-induced mastitis differentially modulate transcriptional responses in neighbouring uninfected bovine mammary gland quarters. *BMC Genomics* **14,** 36.

Jiang, L., Sorensen, P., Rontved, C., Vels, L. &Ingvartsen, K. L. (2008). Gene expression profiling of liver from dairy cows treated intra-mammary with lipopolysaccharide. *BMC Genomics* **9,** 443.

Jin, W., Grant, J. R., Stothard, P., Moore, S. S. &Guan, L. L. (2009). Characterization of bovine miRNAs by sequencing and bioinformatics analysis. *BMC molecular biology* **10,** 90.

Jones, G. M. (2009). Understanding the basics of mastitis. *Virginia Cooperative Extension* **Publication No. 404-233**.

Kanehisa, M., Araki, M., Goto, S., Hattori, M., Hirakawa, M., Itoh, M., *et al.* (2007). KEGG for linking genomes to life and the environment. *Nucleic Acids Res* **36,** D480-4.

Kosaka, N., Izumi, H., Sekine, K. &Ochiya, T. (2010). microRNA as a new immune-regulatory agent in breast milk. *Silence* **1,** 7.

Kozomara, A.Griffiths-Jones, S. (2011). miRBase: integrating microRNA annotation and deep-sequencing data. *Nucleic acids research* **39,** D152-7.

Lawless, N., Foroushani, A. B., McCabe, M. S., O'Farrelly, C. &Lynn, D. J. (2013). Next Generation Sequencing Reveals the Expression of a Unique miRNA Profile in Response to a Gram-Positive Bacterial Infection. *PloS one* **8,** e57543.

Lin, C. Y., Chin, C. H., Wu, H. H., Chen, S. H., Ho, C. W. &Ko, M. T. (2008). Hubba: hub objects analyzer—a framework of interactome hubs identification for network biology. *Nucleic Acids Res* **36,** W438-W443.

Lippolis, J. D., Reinhardt, T. A., Goff, J. P. &Horst, R. L. (2006). Neutrophil extracellular trap formation by bovine neutrophils is not inhibited by milk. *Veterinary Immunology and Immunopathology* **113,** 248-55.

Lynn, D. J., Chan, C., Naseer, M., Yau, M., Lo, R., Sribnaia, A., *et al.* (2010). Curating the innate immunity interactome. *BMC systems biology* **4,** 117.

Lynn, D. J., Winsor, G. L., Chan, C., Richard, N., Laird, M. R., Barsky, A., *et al.* (2008). InnateDB: facilitating systems-level analyses of the mammalian innate immune response. *Mol Syst Biol* **4,** 218.

Ma, J. L., Zhu, Y. H., Zhang, L., Zhuge, Z. Y., Liu, P. Q., Yan, X. D., *et al.* (2011). Serum concentration and mRNA expression in milk somatic cells of toll-like receptor 2, toll-like receptor 4, and cytokines in dairy cows following intramammary inoculation with Escherichia coli. *Journal of Dairy Science* **94,** 5903-12.

Mackowiak, S. D. (2011). Identification of novel and known miRNAs in deep-sequencing data with miRDeep2. *Curr Protoc Bioinformatics* **Chapter 12,** Unit 12 10.

McGettrick, A. F.O'Neill, L. A. (2013). How Metabolism Generates Signals during Innate Immunity and Inflammation. *The Journal of biological chemistry* **288,** 22893-8.

Minakawa, M., Sone, T., Takeuchi, T. &Yokosawa, H. (2008). Regulation of the nuclear factor (NF)-kappaB pathway by ISGylation. *Biological & Pharmaceutical Bulletin* **31,** 2223-7.

Mitterhuemer, S., Petzl, W., Krebs, S., Mehne, D., Klanner, A., Wolf, E., *et al.* (2010). Escherichia coli infection induces distinct local and systemic transcriptome responses in the mammary gland. *BMC Genomics* **11,** 138.

Morris, D., Guerra, C., Donohue, C., Oh, H., Khurasany, M. &Venketaraman, V. (2012). Unveiling the mechanisms for decreased glutathione in individuals with HIV infection. *Clinical & developmental immunology* **2012,** 734125.

Morris, D., Khurasany, M., Nguyen, T., Kim, J., Guilford, F., Mehta, R., *et al.* (2013). Glutathione and infection. *Biochimica et Biophysica Acta* **1830,** 3329-49.

Moser, T. S., Schieffer, D. &Cherry, S. (2012). AMP-activated kinase restricts Rift Valley fever virus infection by inhibiting fatty acid synthesis. *PLoS pathogens* **8,** e1002661.

Moyes, K. M., Drackley, J. K., Morin, D. E., Bionaz, M., Rodriguez-Zas, S. L., Everts, R. E., *et al.* (2009). Gene network and pathway analysis of bovine mammary tissue challenged with Streptococcus uberis reveals induction of cell proliferation and inhibition of PPARgamma signaling as potential mechanism for the negative relationships between immune response and lipid metabolism. *BMC Genomics* **10,** 542.

Mullokandov, G., Baccarini, A., Ruzo, A., Jayaprakash, A. D., Tung, N., Israelow, B., *et al.* (2012). High-throughput assessment of microRNA activity and function using microRNA sensor and decoy libraries. *Nature Methods* **9,** 840-6.

O'Connell, R. M., Rao, D. S., Chaudhuri, A. A. &Baltimore, D. (2010). Physiological and pathological roles for microRNAs in the immune system. *Nature reviews. Immunology* **10,** 111-22.

Porcherie, A., Cunha, P., Trotereau, A., Roussel, P., Gilbert, F. B., Rainard, P., *et al.* (2012). Repertoire of Escherichia coli agonists sensed by innate immunity receptors of the bovine udder and mammary epithelial cells. *Veterinary research* **43,** 14.

Prgomet, C., Sarikaya, H., Bruckmaier, R. M. &Pfaffl, M. W. (2005). Short-term effects on pro-inflammatory cytokine, lactoferrin and CD14 mRNA expression levels in bovine immunoseparated milk and blood cells treated by LPS. *Journal of veterinary medicine. A, Physiology, pathology, clinical medicine* **52,** 317-24.

Reinhardt, T. A., Sacco, R. E., Nonnecke, B. J. &Lippolis, J. D. (2013). Bovine milk proteome: quantitative changes in normal milk exosomes, milk fat globule membranes and whey proteomes resulting from Staphylococcus aureus mastitis. *Journal of proteomics* **82,** 141-54.

Reinoso, E. B., Lasagno, M. C., Dieser, S. A. &Odierno, L. M. (2011). Distribution of virulence-associated genes in Streptococcus uberis isolated from bovine mastitis. *FEMS Microbiology Letters* **318,** 183-8.

Rinaldi, M., Li, R. W. &Capuco, A. V. (2010). Mastitis associated transcriptomic disruptions in cattle. *Veterinary Immunology and Immunopathology* **138,** 267-79.

Robinson, M. D., McCarthy, D. J. &Smyth, G. K. (2010). edgeR: a Bioconductor package for differential expression analysis of digital gene expression data. *Bioinformatics* **26,** 139-40.

Rolland-Turner, M., Goretti, E., Bousquenaud, M., Leonard, F., Nicolas, C., Zhang, L., *et al.* (2013). Adenosine stimulates the migration of human endothelial progenitor cells. Role of CXCR4 and microRNA-150. *PloS one* **8,** e54135.

Rosenberger, C. M., Podyminogin, R. L., Navarro, G., Zhao, G. W., Askovich, P. S., Weiss, M. J., *et al.* (2012). miR-451 regulates dendritic cell cytokine responses to influenza infection. *Journal of Immunology* **189,** 5965-75.

Ross, R. (1999). Atherosclerosis an inflammatory disease. *The New England journal of medicine* **340,** 115-26.

Sandhu, S. K., Volinia, S., Costinean, S., Galasso, M., Neinast, R., Santhanam, R., *et al.* (2012). miR-155 targets histone deacetylase 4 (HDAC4) and impairs transcriptional activity of B-cell lymphoma 6 (BCL6) in the Emu-miR-155 transgenic mouse model. *Proceedings of the National Academy of Sciences of the United States of America* **109,** 20047-52.

Schuster, S. C. (2008). Next-generation sequencing transforms today's biology. *Nature Methods* **5,** 16-8.

Sears, D. D., Hsiao, G., Hsiao, A., Yu, J. G., Courtney, C. H., Ofrecio, J. M., *et al.* (2009). Mechanisms of human insulin resistance and thiazolidinedione-mediated insulin sensitization. *Proceedings of the National Academy of Sciences of the United States of America* **106,** 18745-50.

Serbina, N. V., Jia, T., Hohl, T. M. &Pamer, E. G. (2008). Monocyte-mediated defense against microbial pathogens. *Annual Review of Immunology* **26,** 421-52.

Shannon, P., Markiel, A., Ozier, O., Baliga, N. S., Wang, J. T., Ramage, D., *et al.* (2003). Cytoscape: a software environment for integrated models of biomolecular interaction networks. *Genome Res* **13,** 2498-504.

Sharbati, J., Lewin, A., Kutz-Lohroff, B., Kamal, E., Einspanier, R. &Sharbati, S. (2011). Integrated microRNA-mRNA-analysis of human monocyte derived macrophages upon Mycobacterium avium subsp. hominissuis infection. *PloS one* **6,** e20258.

Shi, C.Pamer, E. G. (2011). Monocyte recruitment during infection and inflammation. *Nature reviews. Immunology* **11,** 762-74.

Swanson, K. M., Stelwagen, K., Dobson, J., Henderson, H. V., Davis, S. R., Farr, V. C., *et al.* (2009). Transcriptome profiling of Streptococcus uberis-induced mastitis reveals fundamental differences between immune gene expression in the mammary gland and in a primary cell culture model. *J Dairy Sci* **92,** 117-29.

Taganov, K. D., Boldin, M. P., Chang, K. J. &Baltimore, D. (2006). NF-kappaB-dependent induction of microRNA miR-146, an inhibitor targeted to signaling proteins of innate immune responses. *Proceedings of the National Academy of Sciences of the United States of America* **103,** 12481-6.

Tannahill, G. M., Curtis, A. M., Adamik, J., Palsson-McDermott, E. M., McGettrick, A. F., Goel, G., *et al.* (2013). Succinate is an inflammatory signal that induces IL-1beta through HIF-1alpha. *Nature* **496,** 238-42.

Tano, N., Kim, H. W. &Ashraf, M. (2011). microRNA-150 regulates mobilization and migration of bone marrow-derived mononuclear cells by targeting Cxcr4. *PloS one* **6,** e23114.

Trapnell, C., Pachter, L. &Salzberg, S. L. (2009). TopHat: discovering splice junctions with RNA-Seq. *Bioinformatics* **25,** 1105-11.

Vaz, C., Ahmad, H. M., Sharma, P., Gupta, R., Kumar, L., Kulshreshtha, R., *et al.* (2010). Analysis of microRNA transcriptome by deep sequencing of small RNA libraries of peripheral blood. *BMC Genomics* **11,** 288.

Venketaraman, V., Dayaram, Y. K., Amin, A. G., Ngo, R., Green, R. M., Talaue, M. T., *et al.* (2003). Role of glutathione in macrophage control of mycobacteria. *Infection and Immunity* **71,** 1864-71.

Ward, J. R., Heath, P. R., Catto, J. W., Whyte, M. K., Milo, M. &Renshaw, S. A. (2011). Regulation of neutrophil senescence by microRNAs. *PLoS One* **6,** e15810.

Ward, P. N., Holden, M. T., Leigh, J. A., Lennard, N., Bignell, A., Barron, A., *et al.* (2009). Evidence for niche adaptation in the genome of the bovine pathogen Streptococcus uberis. *BMC Genomics* **10,** 54.

Wells, S. J., Ott, S. L. &Seitzinger, A. H. (1998). Key health issues for dairy cattle--new and old. *Journal of Dairy Science* **81,** 3029-35.

Whelehan, C. J., Meade, K. G., Eckersall, P. D., Young, F. J. &O'Farrelly, C. (2011). Experimental Staphylococcus aureus infection of the mammary gland induces region-specific changes in innate immune gene expression. *Veterinary Immunology and Immunopathology* **140,** 181-9.

Xu, G., Zhang, Y., Jia, H., Li, J., Liu, X., Engelhardt, J. F., *et al.* (2009). Cloning and identification of microRNAs in bovine alveolar macrophages. *Molecular and cellular biochemistry* **332,** 9-16.

Yamakuchi, M., Ferlito, M. &Lowenstein, C. J. (2008). miR-34a repression of SIRT1 regulates apoptosis. *Proceedings of the National Academy of Sciences of the United States of America* **105,** 13421-6.

Young, M. D., Wakefield, M. J., Smyth, G. K. &Oshlack, A. (2010). Gene ontology analysis for RNA-seq: accounting for selection bias. *Genome biology* **11,** R14.

Yu, H., Kim, P. M., Sprecher, E., Trifonov, V. &Gerstein, M. (2007). The importance of bottlenecks in protein networks: correlation with gene essentiality and expression dynamics. *PLoS computational biology* **3,** e59.

Zimin, A. V., Delcher, A. L., Florea, L., Kelley, D. R., Schatz, M. C., Puiu, D., *et al.* (2009). A whole-genome assembly of the domestic cow, Bos taurus. *Genome biology* **10,** R42.

Figure Legends

Figure 1. Overview of the experimental design. Five Holstein Friesian animals were infected via the teat canal of the right front quarter with approximately 500 CFU of a mastitis-causing pathogen, *Streptococcus uberis* 0140, in 10 ml of saline. Five control animals were inoculated with saline only. Milk and blood samples were obtained from each animal at 0, 12, 24, 36 and 48 hrs post-infection (or mock infection). Milk and blood derived CD14+ monocytes were isolated by Fluorescence-activated cell sorting (FACS) from each sample. mRNA and miRNA were extracted and 200 Illumina-compatible libraries were prepared for sequencing on a HiSeq 2000 machine. More than 4 billion mRNA reads and > 2 billion miRNA reads were sequenced in total.

Figure 2. The response to infection. A) The infection was monitored using recorded milk bacterial counts (CFU/ml) and B) somatic cell counts (per ml) at each of the five time points (0, 12, 24, 36 and 48hpi) for each animal (control & infected). Significant heterogeneity was observed in the CFU data among the infected animals. One infected animal (TI2) was observed to have only a very modest increase in bacterial counts. C-F) Hierarchical clustering of top 500 most variable probes in milk-isolated monocytes (MIMs) at 12, 24, 36 and 48hpi, respectively, revealed that infected animals separated from control animals in their gene expression response at 36 and 48hpi except for animal TI2. G-J) InnateDB network analysis of genes that were differentially expressed at 12, 24, 36 and 48hpi, respectively. The networks were visualised in Cytoscape.

Figure 3. Pathways that were statistically overrepresented among genes. A) up-regulated at 36hpi; B) up-regulated at 48hpi; C) down-regulated at 36hpi; D) down-regulated at 48hpi; in MIMs isolated from *S. uberis* infected animals. Up-regulated genes were significantly enriched for roles in inflammatory and other innate immune pathways, while down-regulated genes were significantly associated with metabolic pathways.

Figure 4. Differential gene expression in key innate immune pathways in MIMs from *S. uberis* infected animals. A-C) Differentially expressed genes highlighted on KEGG Toll-like receptor (TLR), NOD-like receptor (NLR), and RIG-I signalling pathway diagrams (Red = up-regulated; Green = down-regulated). D-F) RPKM values for each of the differentially expressed genes in the TLR, NLR and RIG-I pathways, respectively (Red = infected; Blue = Control). C) Fold change values for each of the differentially expressed genes in the TLR, NLR and RIG-I pathways, respectively (Red = up-regulated; Green = down-regulated).

Figure 5. Network analysis of differentially expressed genes. InnateDB was used to generate a network of experimentally-supported molecular interactions that have been annotated to occur directly between the differentially expressed genes and their encoded products. A) The top 20 CytoHubba-predicted network hubs and their interactors. Overlain on the network is gene expression data from MIMs at 36hpi (Red = up-regulated; Green = down-regulated). The top 20 hubs were highly enriched for roles in innate immunity. B) The high-scoring differentially expressed sub-network identified in the larger network using jActiveModules. This module was highly enriched for several innate immune relevant pathways.

Figure 6. A heatmap of the normalised read counts of miRNAs that were identified as differentially expressed in MIMs at 36hpi. Hierarchical clustering revealed the separation of the infected and control animals based on this miRNA expression data. Note that one infected animal (TI2) is not included in this analysis as it did not appear to respond to the infection as measured by CFU or mRNA expression data (see Figure 2).

Figure 7. Visualization of miRNA targets. A) Two-dimensional cluster analysis and heatmap visualization of the miRNA/mRNA expression correlation data matrix after filtering by predicted miRNA-targets and correlation significance. The primary split in the upper hierarchical dendrogram largely aligns with the up-regulated miRNA (red) and down-regulated miRNA (green). miRNA/mRNA target expression correlations are coloured based on increasing significance (light blue to blue) with non-target/non-significant correlations masked (grey). B) A network representation of the predicted targets (circular nodes) of down-regulated miRNAs (green arrows). Red circles = up-regulated in MIM mRNA expression data at either 36 and/or 48hpi. Larger circular nodes represent those genes which have been annotated by InnateDB to have a role in innate immunity. C) A network representation of the predicted targets (circular nodes) of up-regulated miRNAs (red arrows). Green circles = down-regulated in MIM mRNA expression data at either 36 and/or 48hpi. Note that the predicted targets of down-regulated but not up-regulated miRNAs are highly enriched for roles in innate immunity.

Tables

Tissue	Hours post infection (hpi)	miR Name	Fold change	FDR
MIMs	12	bta-miR-615	16.53	0.002591533
MIMs	12	bta-miR-451	32.73	0.022589776
MIMs	12	bta-miR-486	1.77	0.051194817
MIMs	36	bta-miR-34a	-8.07	0.003853138
MIMs	36	bta-miR-200c	-7.12	0.021524752
MIMs	36	bta-miR-200b	-6.59	0.022403054
MIMs	36	bta-miR-182	-6.43	0.034621112
MIMs	36	bta-miR-125a	-5.86	0.000854468
MIMs	36	bta-miR-200a	-4.90	0.061309129
MIMs	36	bta-let-7e	-4.51	0.046884171
MIMs	36	bta-miR-760-3p	-4.38	0.030789676
MIMs	36	bta-miR-193a-5p	-4.13	0.099288316
MIMs	36	bta-miR-150	-4.05	0.014886528
MIMs	36	bta-miR-210	-4.03	0.000399613
MIMs	36	bta-miR-375	-3.88	0.021524752
MIMs	36	bta-miR-149-5p	-2.77	0.099288316
MIMs	36	bta-miR-30a-5p	-2.48	0.046884171
MIMs	36	bta-miR-142-5p	2.21	0.033031656
MIMs	36	bta-miR-363	2.23	0.049537718
MIMs	36	bta-miR-223	2.44	0.011440656
MIMs	36	bta-miR-338	2.51	0.017723606
MIMs	36	bta-miR-339a	2.82	0.01613752
MIMs	36	bta-miR-2898	2.98	0.003853138
MIMs	36	bta-miR-1291	3.07	0.033031656
MIMs	36	bta-miR-423-5p	5.73	0.014512876
MIMs	36	bta-miR-451	47.12	6.28E-07
MIMs	48	bta-let-7e	-6.92	0.055709133
MIMs	48	bta-miR-200b	-6.06	0.055709133
MIMs	48	bta-miR-34a	-5.37	0.014991858
MIMs	48	bta-miR-149-5p	-4.01	0.055709133
MIMs	48	bta-miR-375	-3.76	0.006976206
MIMs	48	bta-miR-210	-3.39	0.072510577
MIMs	48	bta-miR-125a	-3.29	0.087523866
MIMs	48	bta-miR-150	-3.18	0.033651802
MIMs	48	bta-miR-99b	-2.9	0.055709133
MIMs	48	bta-miR-338	2.81	0.055709133
MIMs	48	bta-miR-486	12.79	0.006655283
MIMs	48	bta-miR-451	48	1.79E-05
BIMs	24	bta-miR-146b	-23.26	0.023903261
BIMs	48	bta-miR-451	9.74	0.067032312
BIMs	48	bta-miR-146b	-3.52	0.067032312
BIMs	48	bta-miR-411a	-22.44	0.067032312

Table 1. Fold changes and false discovery rates of differentially expressed miRNAs at 12, 24, 36, and 48 hours post-infection in milk and blood isolated monocytes.

Supplementary Information

File S1. 1.1 MirVanaTM RNA Isolation Kit protocol, 1.2 MirPremierTM microRNA Isolation Kits protocol, 1.3 TruSeq RNA Sample Preparation Kit v2 (50 cycles), 1.4 TruSeq Small RNA Sample Preparation Kit (50 cycles), 1.5 RNA integrity and quantification, 1.6 References.

Figure S1. Heatmap of differential gene expression (tpm) in blood isolated monocytes across infected and control animals at 12, 24, 36, & 48hpi. The more red the colour the more highly expressed that gene is, R (V2.15.2) hclust package.

Figure S2. Down-regulated genes highlighted on the KEGG metabolism network.

Figure S3. The proportion of reads aligning uniquely to bovine ncRNAs. A) Reads aligning to ncRNAs in milk isolated monocytes. B) Reads aligning to ncRNAs in blood isolated monocytes. The majority of reads align to known miRNAs.

Table S1. Manually generated pathway annotations for inflammasome and interferon pathways sourced from SA biosciences (Qiagen) RT² Profiler™ PCR Array Human Interferon and Receptors (PAHS-064A), and RT² Profiler™ PCR Array Human Inflammasome (PAHS-097A) annotations.

Table S2. Summary read statistics and number of unique alignments for each RNA and miRNA library.

Table S3. Summary of milk volumes, rectal temperatures, ambient temperatures, humidity, and bacterial CFU counts for each animal. Summary of total cell counts, FACS isolated cell numbers, RNA integrity, quantity, 18/28S ratio, total quantity of RNA/miRNA for each of the 100 RNA/miRNA samples.

Table S4. Average correlation coefficients of mRNA normalised read counts between samples at each time-point for control and infected biological replicates. Calculations were carried out in R (version 2.15.2).

Table S5. Differentially expressed genes in milk and blood isolated monocytes at 12, 24, 36, and 48 hours post infection.

Table S6. Significantly over-represented KEGG pathways among differentially expressed genes in milk and blood isolated monocytes at 12, 24, 36, & 48 hours post infection.

Table S7. The top 20 network hubs identified using CytoHubba and enriched Gene Ontology terms among hubs.

Table S8. The top 20 contextual hubs identified using the CHAT software.

Table S9. Significantly over-represented KEGG pathways among genes identified in the jActiveModules module.

Table S10. miRNAs that are expressed ≥ 1 tag per million in bovine blood and milk isolated monocytes.

Table S11. Summary of co-expression, target analysis, and Pearson correlations of miRNA and mRNA data.

Table S12. Significantly over-represented KEGG pathways among predicted miRNA targets.

Table S13. Putative novel bovine miRNAs discovered through miRDeep2 analysis of miRNAseq data from 100 milk and blood isolated monocytes.

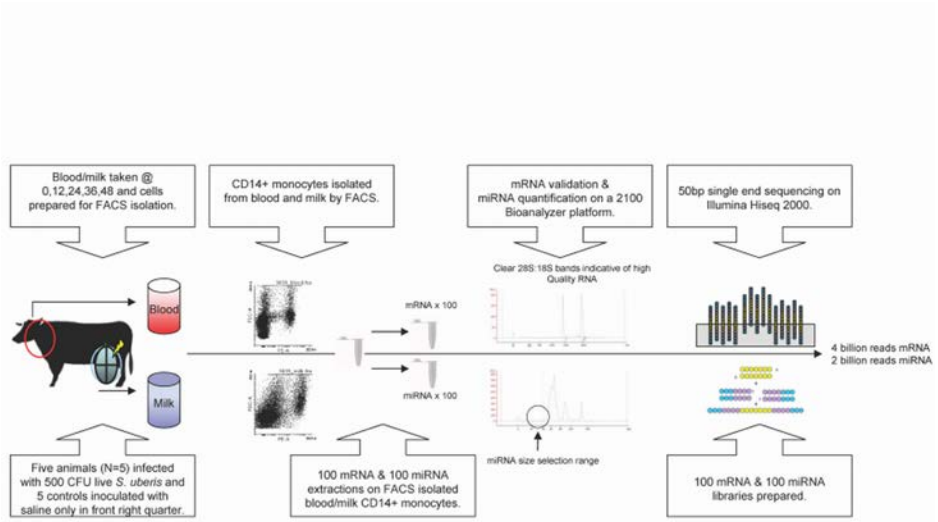
Blood/milk taken @ 0,12,24,36,48 and cells prepared for FACS isolation.
CD14+ monocytes isolated from blood and milk by FACS.
mRNA validation & miRNA quantification on a 2100 Bioanalyzer platform.
50bp single end sequencing on Illumina Hiseq 2000.
Clear 28S:18S bands indicative of high Quality RNA
Blood
Milk
mRNA x 100
mRNA x 100
4 billion reads mRNA
2 billion reads miRNA
miRNA size selection range
Five animals (N=5) infected with 500 CFU live S. uberis and 5 controls inoculated with saline only in front right quarter.
100 mRNA & 100 miRNA extractions on FACS isolated blood/milk CD14+ monocytes.
100 mRNA & 100 miRNA libraries prepared.

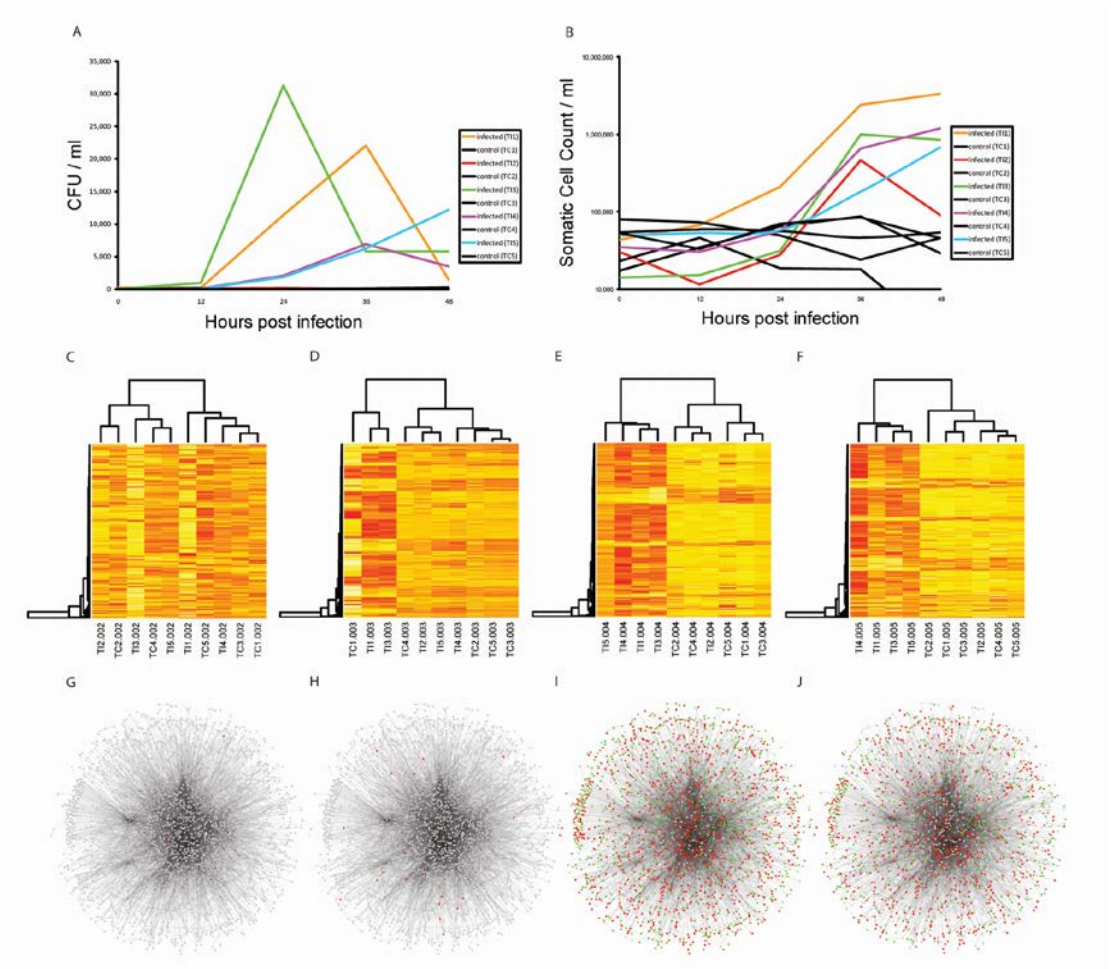
A
CFU / ml
Hours post infection
B
Somatic Cell Count / ml
Hours post infection
C
D
E
F
G
H
I
J

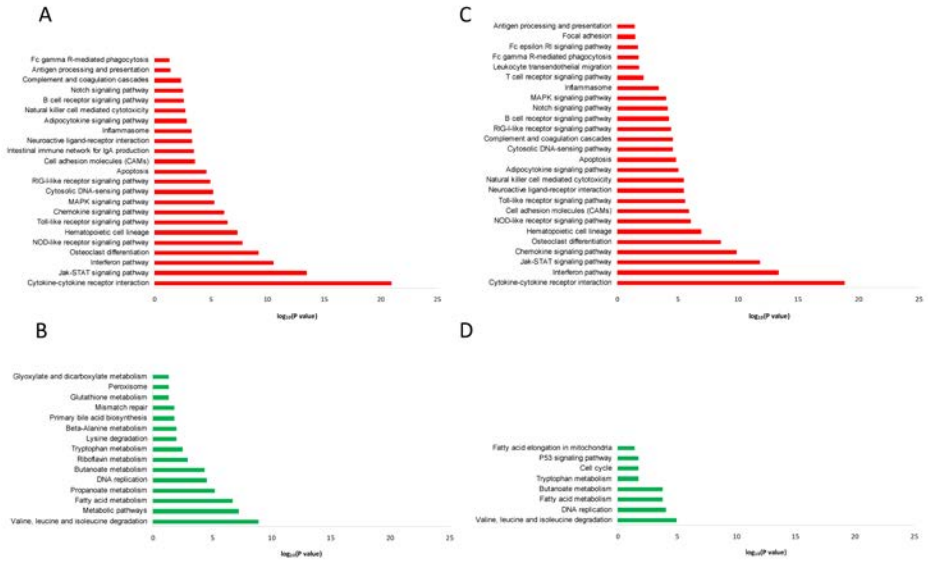
A
Fc gamma R-mediated phagocytosis
Antigen processing and presentation
Complement and coagulation cascades
Notch signaling pathway
B cell receptor signaling pathway
Natural killer cell mediated cytotoxicity
Adipocytokine signaling pathway
Inflammasome
Neuroactive ligand-receptor interaction
Intestinal immune network for IgA production
Cell adhesion molecules (CAMs)
Apoptosis
RIG-I-like receptor signaling pathway
Cytosolic DNA-sensing pathway
MAPK signaling pathway
Chemokine signaling pathway
Toll-like receptor signaling pathway
Hematopoietic cell lineage
NOD-like receptor signaling pathway
Osteoclast differentiation
Interferon pathway
Jak-STAT signaling pathway
Cytokine-cytokine receptor interaction
0
5
10
15
20
25
log10(P value)
C
Antigen processing and presentation
Focal adhesion
Fc epsilon RI signaling pathway
Fc gamma R-mediated phagocytosis
Leukocyte transendothelial migration
T cell receptor signaling pathway
Inflammasome
MAPK signaling pathway
Notch signaling pathway
B cell receptor signaling pathway
RIG-I-like receptor signaling pathway
Complement and coagulation cascades
Cytosolic DNA-sensing pathway
Apoptosis
Adipocytokine signaling pathway
Natural killer cell mediated cytotoxicity
Neuroactive ligand-receptor interaction
Toll-like receptor signaling pathway
Cell adhesion molecules (CAMs)
NOD-like receptor signaling pathway
Hematopoietic cell lineage
Osteoclast differentiation
Chemokine signaling pathway
Jak-STAT signaling pathway
Interferon pathway
Cytokine-cytokine receptor interaction
0
5
10
15
20
25
log10(P value)
B
Glyoxylate and dicarboxylate metabolism
Peroxisome
Glutathione metabolism
Mismatch repair
Primary bile acid biosynthesis
Beta-Alanine metabolism
Lysine degradation
Tryptophan metabolism
Riboflavin metabolism
Butanoate metabolism
DNA replication
Propanoate metabolism
Fatty acid metabolism
Metabolic pathways
Valine, leucine and isoleucine degradation
0
5
10
15
20
25
log10(P value)
D
Fatty acid elongation in mitochondria
P53 signaling pathway
Cell cycle
Tryptophan metabolism
Butanoate metabolism
Fatty acid metabolism
DNA replication
Valine, leucine and isoleucine degradation
0
5
10
15
20
25
log10(P value)

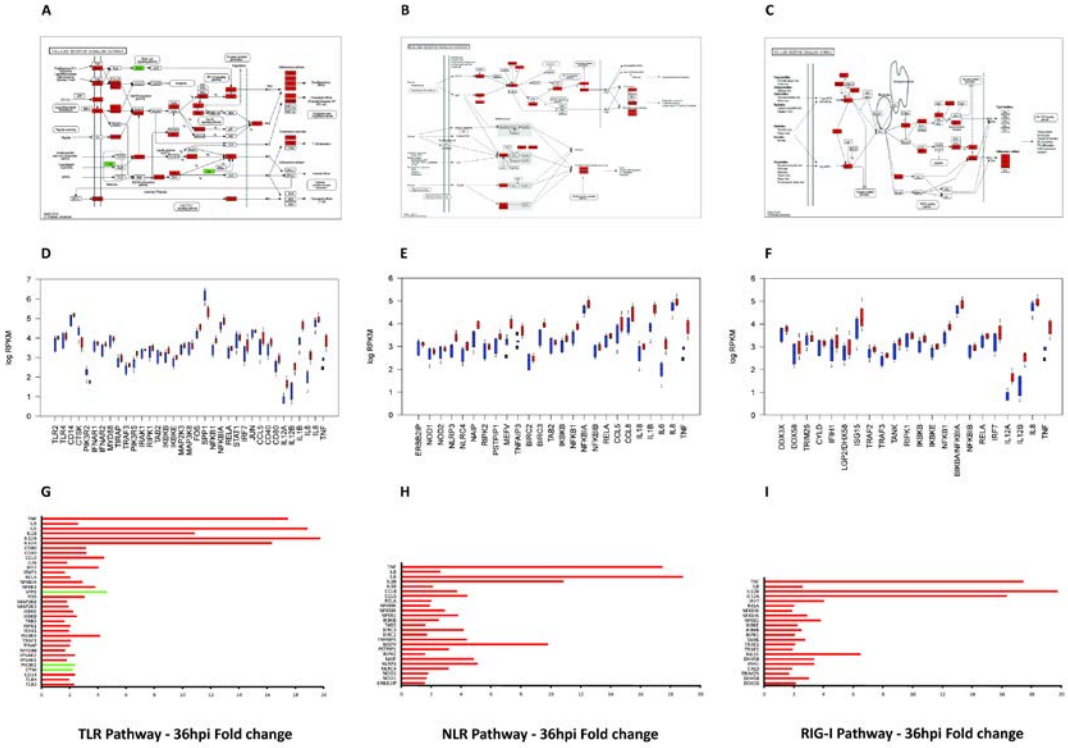

TLR Pathway - 36hpi Fold change

NLR Pathway - 36hpi Fold change

RIG-I Pathway - 36hpi Fold change

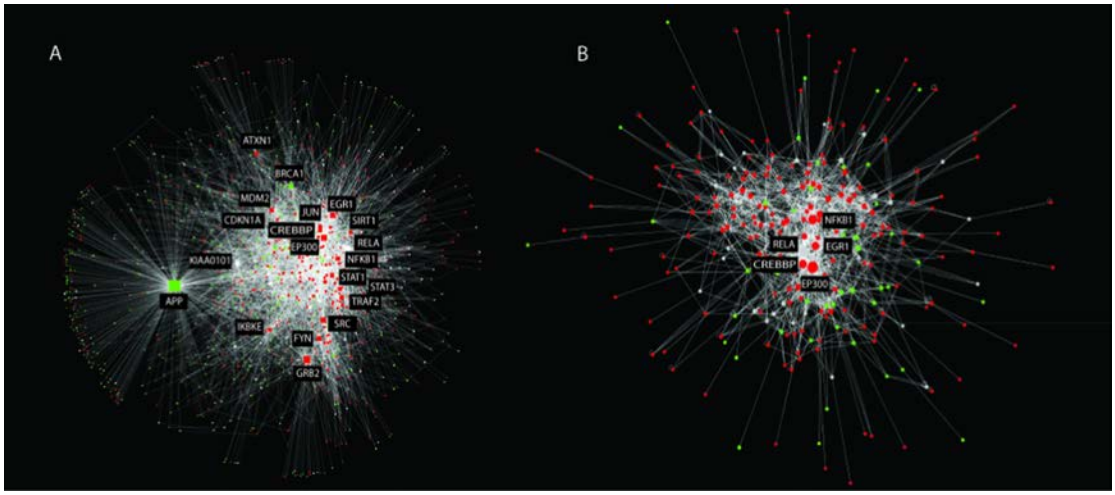
A
B
ATXN1
BRCA1
MDM2
JUN
EGR1
CDKN1A
CREBBP
SIRT1
RELA
EP300
NFKB1
KIAA0101
STAT1
STAT3
APP
TRAF2
IKBKE
SRC
FYN
GRB2
NFKB1
RELA
EGR1
CREBBP
EP300

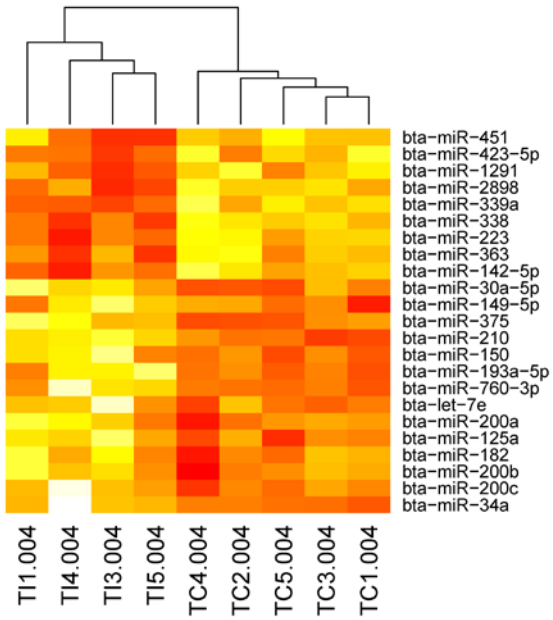
bta-miR-451
bta-miR-423-5p
bta-miR-1291
bta-miR-2898
bta-miR-339a
bta-miR-338
bta-miR-223
bta-miR-363
bta-miR-142-5p
bta-miR-30a-5p
bta-miR-149-5p
bta-miR-375
bta-miR-210
bta-miR-150
bta-miR-193a-5p
bta-miR-760-3p
bta-let-7e
bta-miR-200a
bta-miR-125a
bta-miR-182
bta-miR-200b
bta-miR-200c
bta-miR-34a
TI1.004
TI4.004
TI3.004
TI5.004
TC4.004
TC2.004
TC5.004
TC3.004
TC1.004

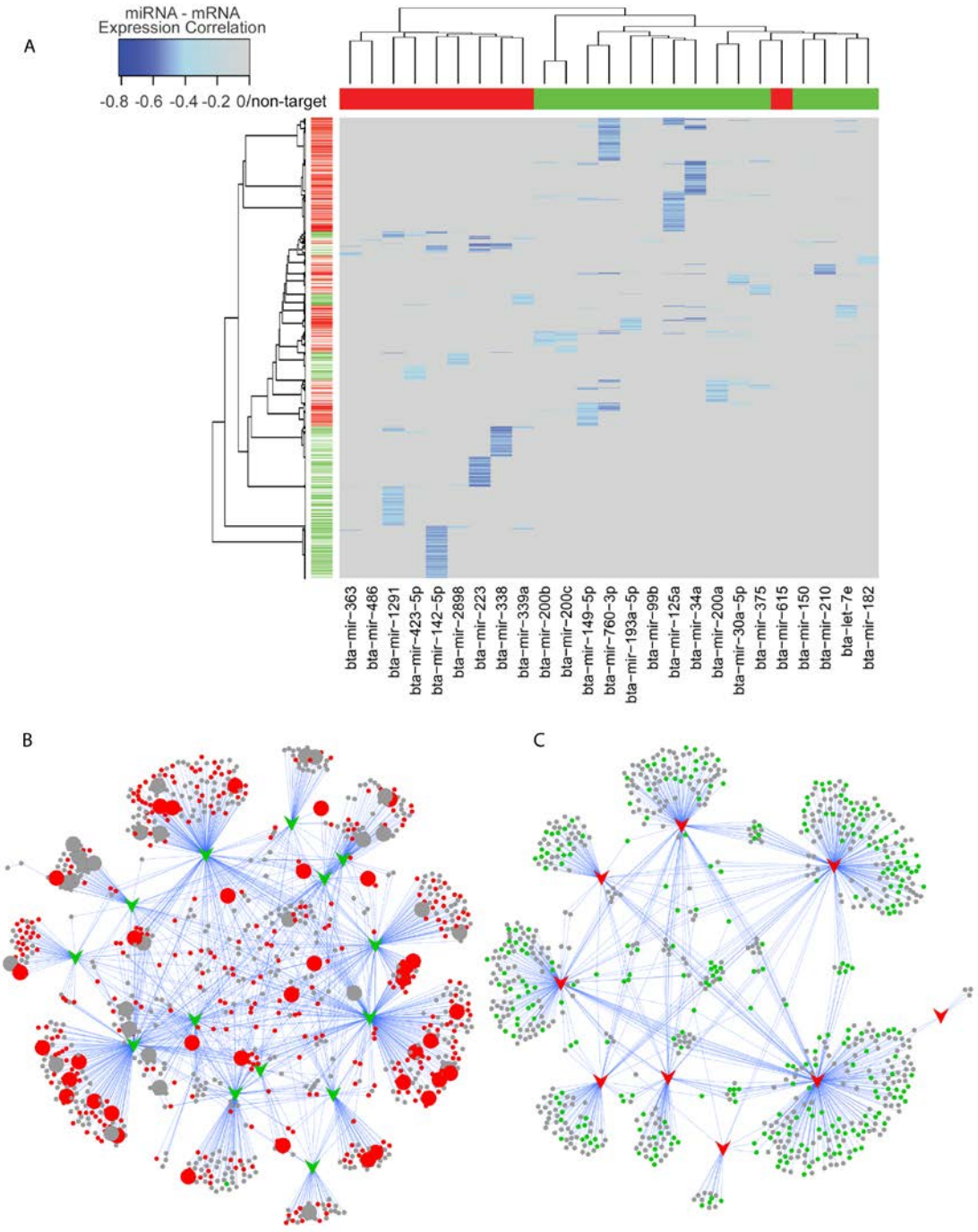
A
miRNA - mRNA
Expression Correlation
-0.8 -0.6 -0.4 -0.2 0/non-target
bta-mir-363
bta-mir-486
bta-mir-1291
bta-mir-423-5p
bta-mir-142-5p
bta-mir-2898
bta-mir-223
bta-mir-338
bta-mir-339a
bta-mir-200b
bta-mir-200c
bta-mir-149-5p
bta-mir-760-3p
bta-mir-193a-5p
bta-mir-99b
bta-mir-125a
bta-mir-34a
bta-mir-200a
bta-mir-30a-5p
bta-mir-375
bta-mir-615
bta-mir-150
bta-mir-210
bta-let-7e
bta-mir-182
B
C